

# The parameterization of subgrid scale orography in LMDz

**François Lott, LMD/CNRS, Ecole Normale Supérieure, Paris**

[flott@lmd.ens.fr](mailto:flott@lmd.ens.fr)

P. Baines, L. Guez, F. Hourdin, L. Fairhead, P. Levan, M. Miller,  
S. Mailler, T. Palmer

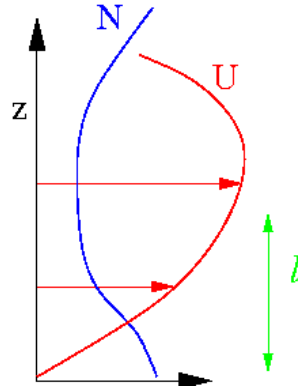
- 1) Linear theory
- 2) Nonlinear effects and breaking
- 3) Formulation of a SSO parameterization
- 4) Validation and test in a NWP model
- 5) Impact in a GCM
- 6) Prospective

# The parameterization of subgrid scale orography in LMDz

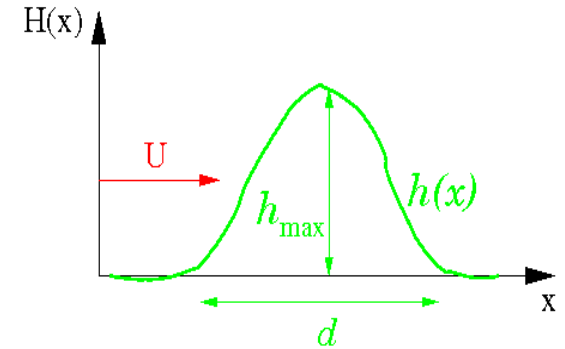
## 1) Linear theory

Dimensional analysis:

Background flow parameters  
 $N, U, l$ , (and  $f$ )



Mountain dimensions  
 $d$  and  $h$



Param. controlling the linear dynamics:

and low level « trapped waves »:

$$Fr^{-1} = \frac{N d}{U}$$

$$Ro^{-1} = \frac{f d}{U}$$

$$L = \frac{N l}{U}$$

Param. controlling the non-linear dynamics:

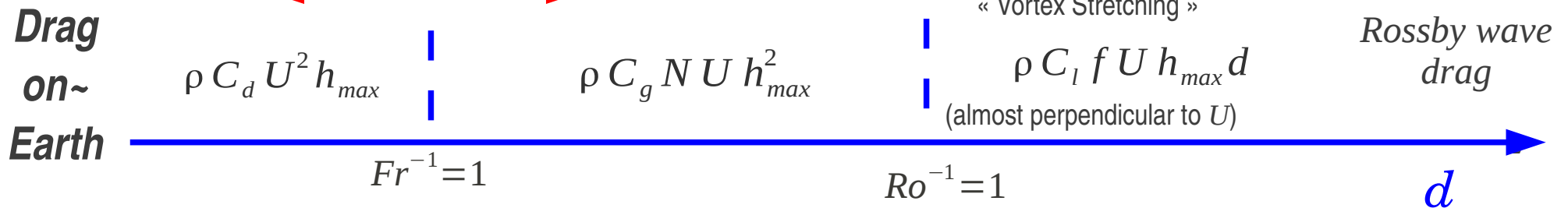
$$S = \frac{h_{max}}{d}$$

$$H_{ND} = \frac{N h_{max}}{U}$$

Boundary layer dynamics

Mesoscale dynamics (incl. Gravity waves)

Synoptic scale and planetary scale dynamics



# The parameterization of subgrid scale orography in LMDz

## 1) Linear theory

In the linear case the response to the mountain can be analysed in terms of Fourier series

(here for a periodic domain  $-X < x < X$ , and for  $U$  and  $N$  constant)

$$h(x) = \sum_{K=0}^M \hat{h}_K \cos\left(K \frac{\pi}{X} x + \chi_K\right), \hat{h}_K = \frac{1}{X} \int_{-X}^X h(x) \cos\left(K \frac{\pi}{X} x + \chi_K\right) dx$$

Giving the vertical velocity:

$$w(x, z) = - \sum_{K=1}^{K_f-1} kU \hat{h}_K e^{-m_K z} \sin(kx + \chi_K) - \sum_{K=K_f}^{K_N} \hat{h}_K \sin(m_K z + kx + \chi_K) - \sum_{K=K_N+1}^M kU \hat{h}_K e^{-m_K z} \sin(kx + \chi_K)$$

Evanescent « long »  
disturbances

$$(K_f \approx 4\pi \frac{fX}{U})$$

Gravity waves

Evanescent « short »  
disturbances

$$(K_N \approx 4\pi \frac{NX}{U})$$

$$m_k = +k \sqrt{\left| \frac{N^2 - k^2 U^2}{k^2 U^2 - f^2} \right|}$$

Vertical scale of variation

Heuristic linear analysis, prediction for the mountain drag:

$$Dr = \frac{1}{2X} \int_{-X}^{+X} p \frac{dh}{dx} = \frac{1}{2} \sum_{K=K_f}^{K_N} \rho(0) \sqrt{|(N^2 - k^2 U^2)(k^2 U^2 - f^2)|} \hat{h}_K^2$$

Only the gravity waves contribute to the drag!

# The parameterization of subgrid scale orography in LMDz

## 1) Linear theory

The 2D linear analysis of Queney (1947), mountain drag:

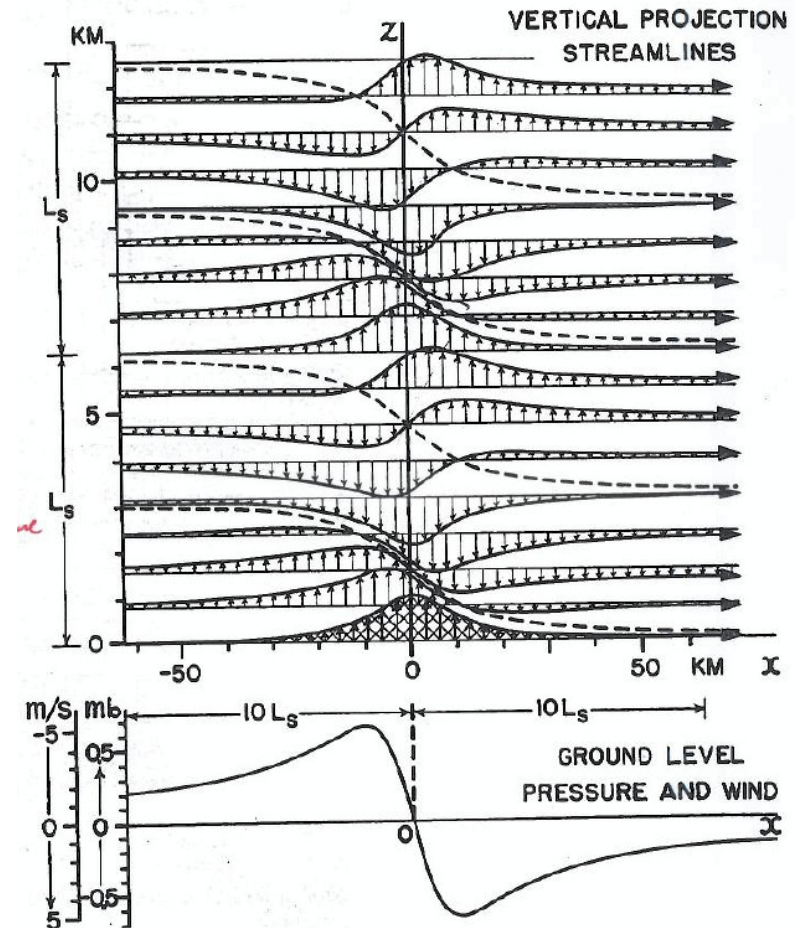
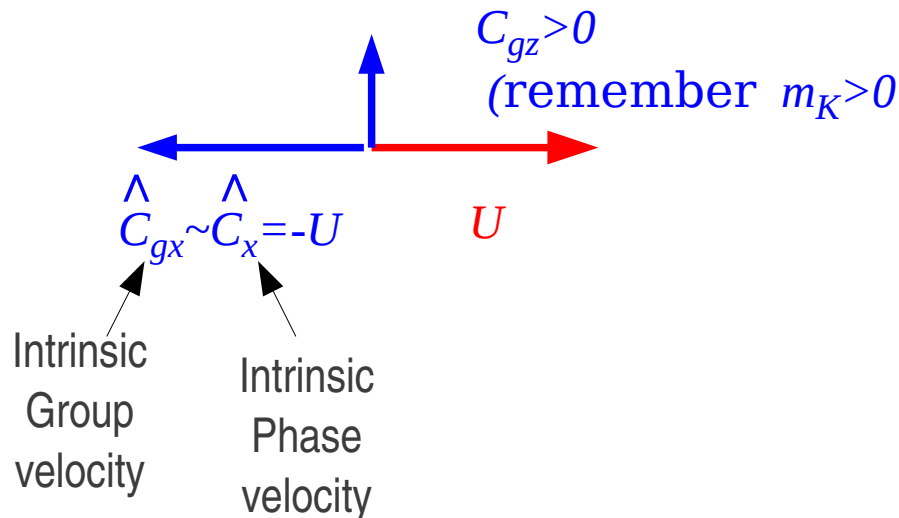
$$U=10\text{m/s}, N=0.01\text{ s}^{-1}, f=10^{-4}\text{ s}^{-1}$$

$$Dr = \frac{1}{2X} \int_{-X}^X p \frac{dh}{dx} dx$$

$$h(x) = \frac{h_{max}}{1 + \frac{x^2}{d}}$$

Case (a):

$d=10\text{km}$ , non rotating and hydrostatic



# The parameterization of subgrid scale orography in LMDz

## 1) Linear theory

The 2D linear analysis of Queney (1947), mountain drag:

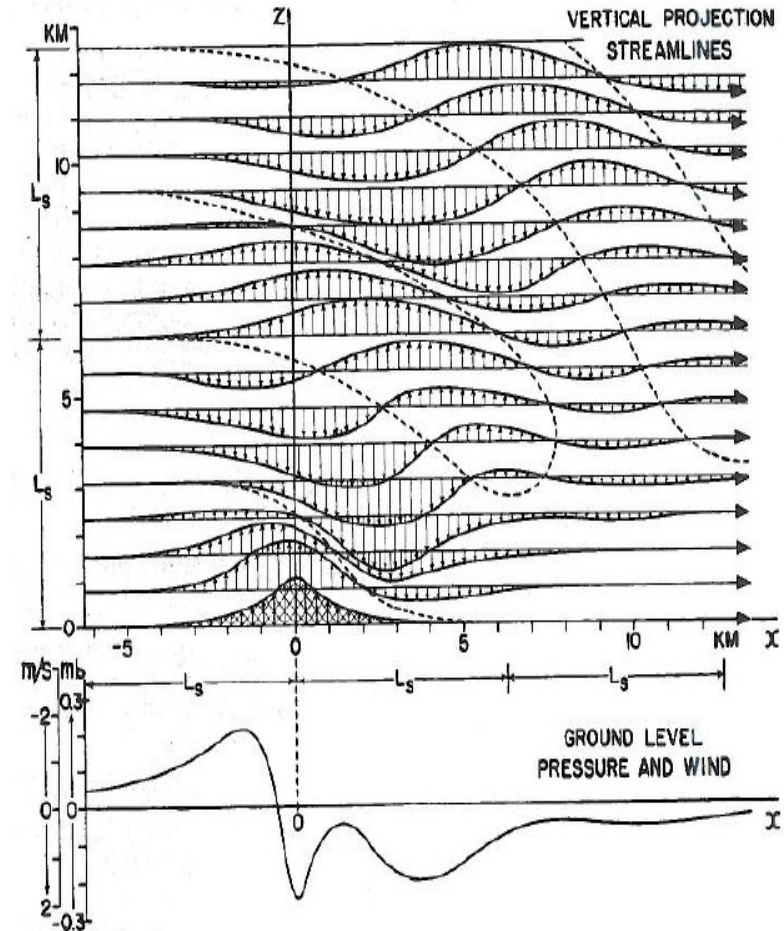
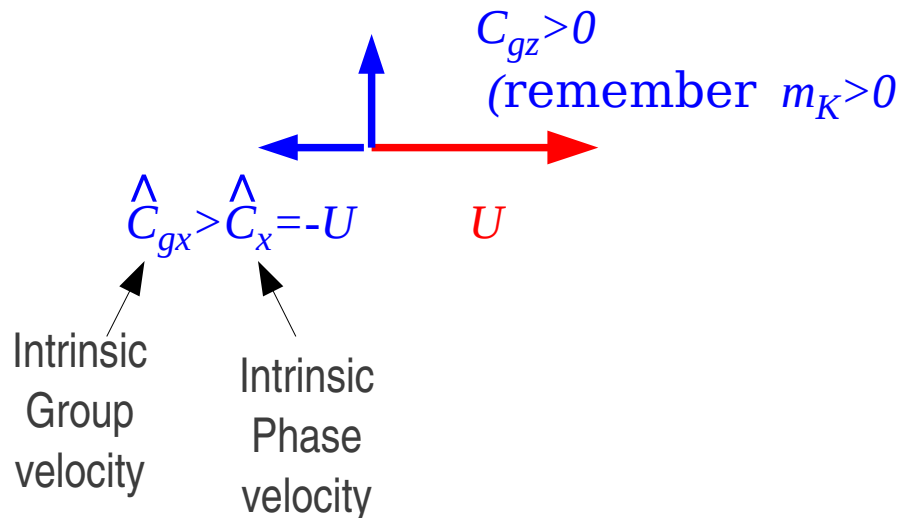
$$U=10\text{m/s}, N=0.01\text{ s}^{-1}, f=10^{-4}\text{ s}^{-1}$$

$$Dr = \frac{1}{2X} \int_{-X}^X p \frac{dh}{dx} dx$$

$$h(x) = \frac{h_{max}}{1 + \frac{x^2}{d}}$$

Case (b):

$d=1\text{km}$ , non-hydrostatic, non-rotating



# The parameterization of subgrid scale orography in LMDz

## 1) Linear theory

The 2D linear analysis of Queney (1947), mountain drag:

$$U=10\text{m/s}, N=0.01 \text{ s}^{-1}, f=10^{-4} \text{ s}^{-1}$$

$$Dr = \frac{1}{2X} \int_{-X}^X p \frac{dh}{dx} dx$$

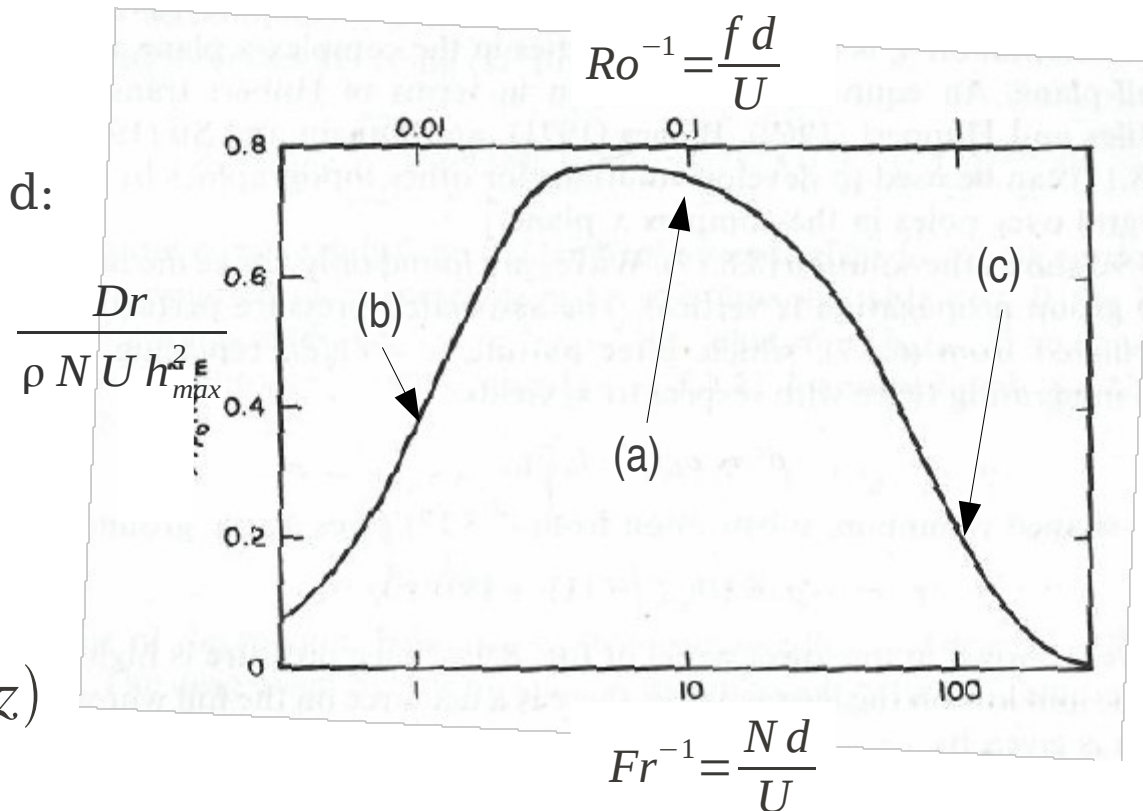
$$h(x) = \frac{h_{max}}{1 + \frac{x^2}{d}}$$

Results for the drag as a function of  $d$ :

In the linear steady undissipative periodic case, for all altitudes  $z$ :

$$Dr = -\frac{1}{2X} \int_{-X}^X \rho u' w' dx = \bar{F}^z(z)$$

Eliassen-Palm (1961) theorem



# The parameterization of subgrid scale orography in LMDz

## 1) Linear theory

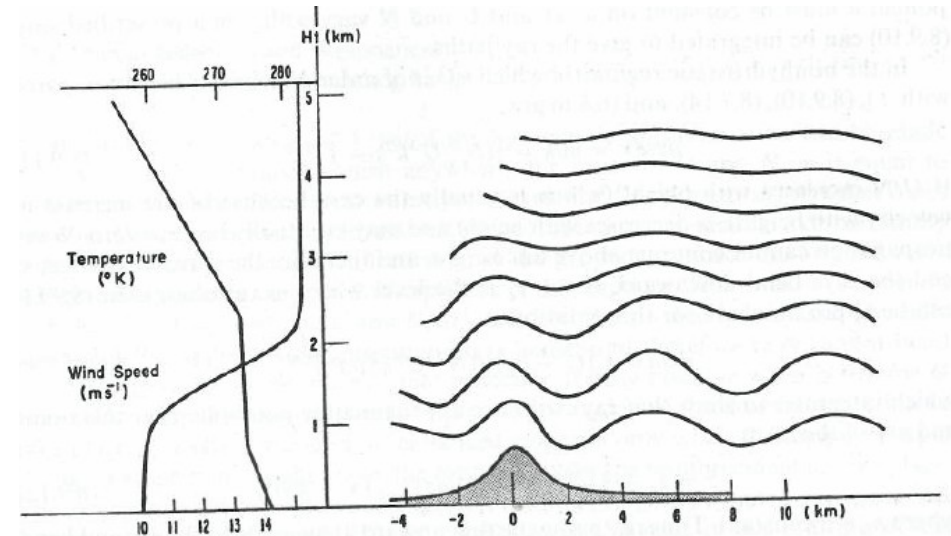
Trapped lee-waves and critical levels ( $U(z)$  and  $N(z)$  varies)

2D-Boussinesq linear non-rotating theory

$$\frac{\partial^2 \hat{w}}{\partial z^2} + \left( \frac{N^2}{U^2} - \frac{U_{zz}}{U} - k^2 \right) \hat{w} = 0$$

$S(z)$   
Scorer  
parameter

$$w(x, z) = \int_{-\infty}^{\infty} \hat{w}(k, z) e^{ikx} dk$$



Scorer (1949) + Gossard and Hooke (1975)

WKB theory:  $m_k^2(z) = S(z) - k^2$

Critical level  $S(z_c) = \infty, U(z_c) = 0$

WKB theory predicts:  $\lim_{z \rightarrow z_c} m_k(z) \rightarrow \infty$

Breaking and/or dissipation below  $z_c$

Turning height:  $S(z_c) - k^2 = 0$

WKB theory predicts  $\lim_{z \rightarrow z_c} m_k(z) \rightarrow 0$

Total or partial reflection around  $z_c$

Free modes such that  $w(k, z=0) = 0$  can be resonantly excited leading to trapped lee

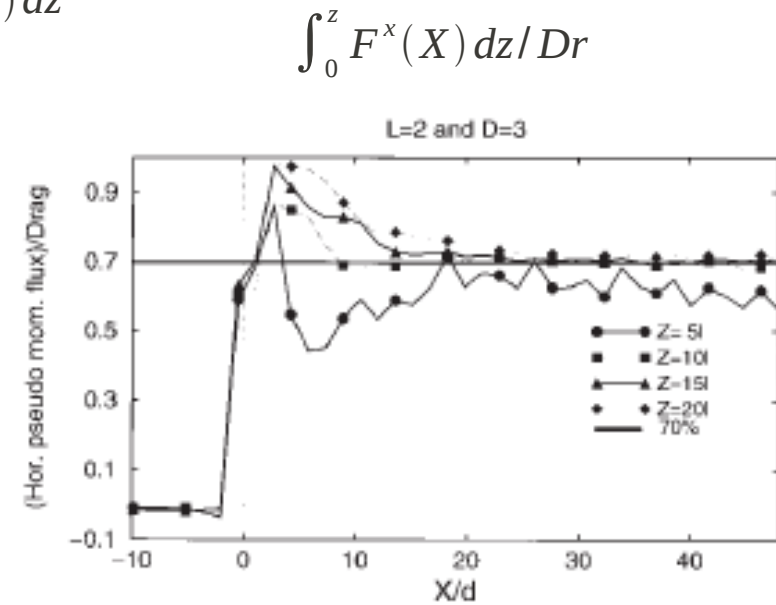
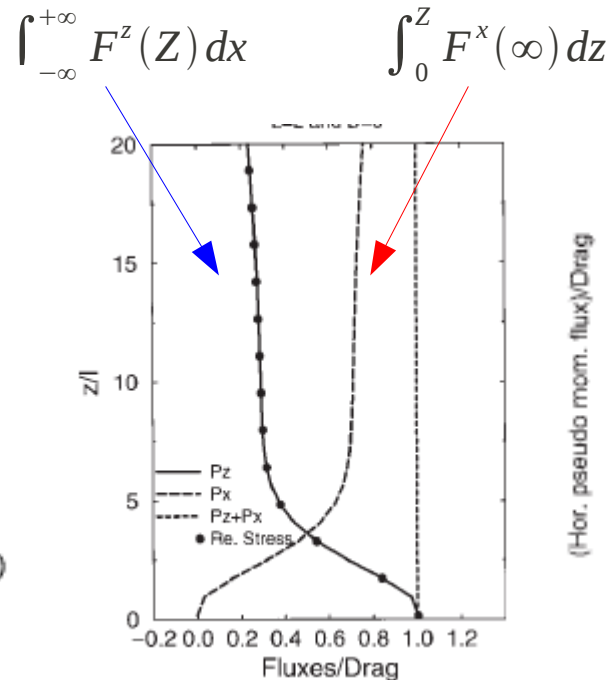
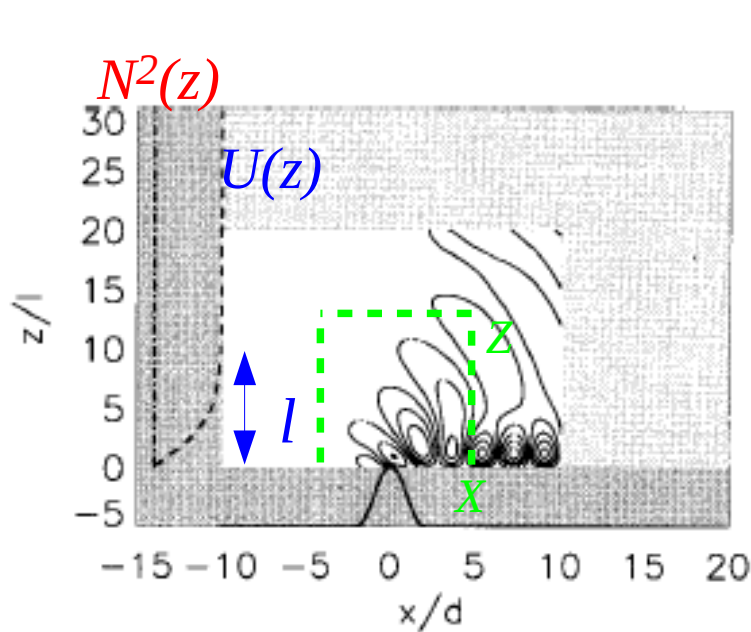
waves

# The parameterization of subgrid scale orography in LMDz

## 1) Linear theory

The general wave action law integrated over a non periodic domain in the steady undissipative case gives:

$$\int_{-X}^{+X} F^z(Z) dx + \int_0^Z F^x(X) dz = Dr$$



The trapped lee waves can transport downstream and at low level a substantial fraction of the mountain drag



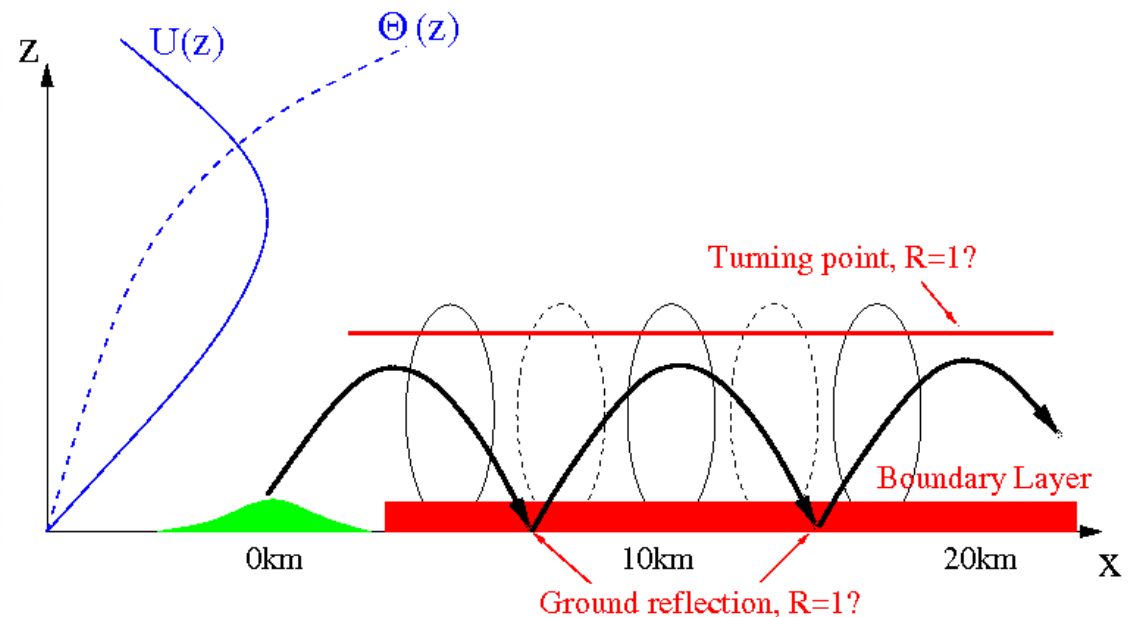
# The parameterization of subgrid scale orography in LMDz

## 1) Linear theory

### Trapped lee-waves and boundary layers



Gravity waves trapping and lee waves (Scorer 1949)



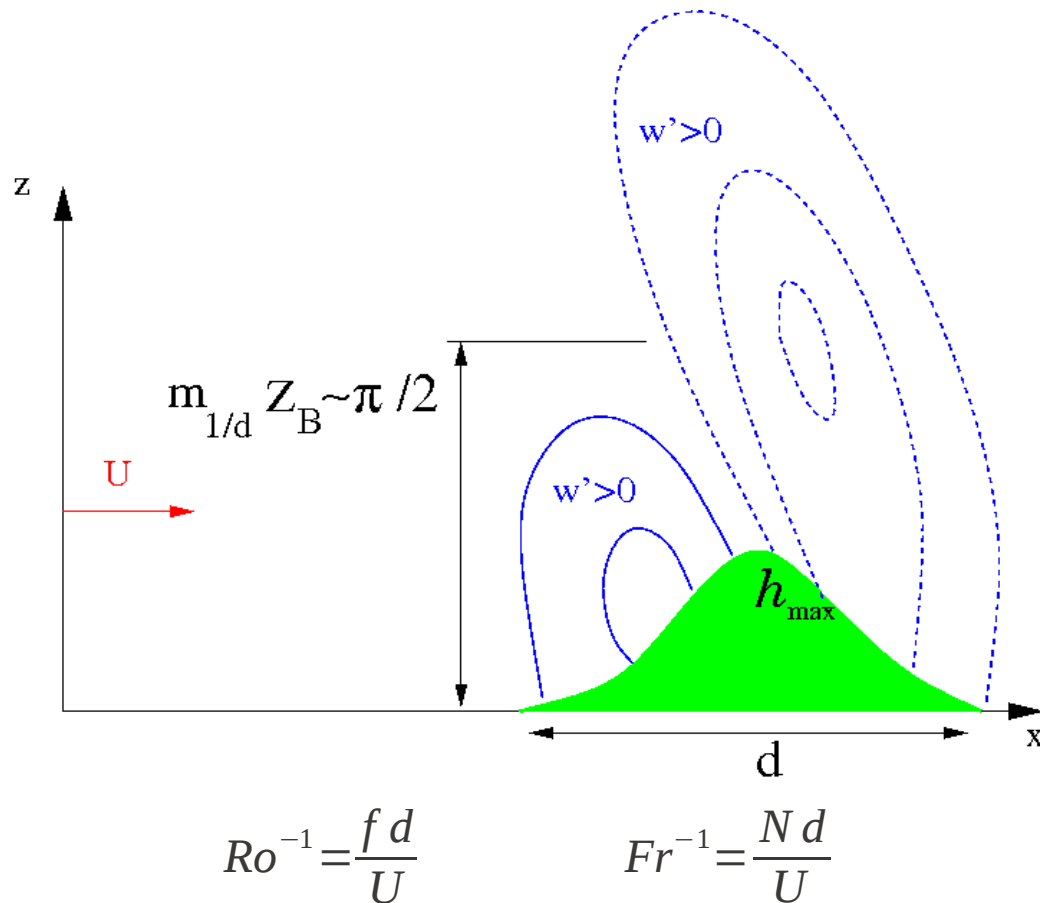
Observations (like during MAP, 1999) have shown that the existence of a turning point aloft is not a sufficient condition for the existence of trapped lee-waves. The conventional linear theory assumes perfect ground reflection, which can be very wrong when there is a boundary layer. (Smith et al. 2002, 2006, Lott 2007).

# The parameterization of subgrid scale orography in LMDz

## 2) Non-linear effects and breaking

Heuristic definition of a « Blocking Height »

$$Z_B$$



Linearity condition :  $Z_B \gg h_{max}$

From the vertical wavenumber definition:

$$m_k = +k \sqrt{\left| \frac{N^2 - k^2 U^2}{k^2 U^2 - f^2} \right|}$$

$Z_B$  can be written:

$$Z_B \sim \frac{\pi}{2 m_{1/d}} = \frac{\pi d}{2} \sqrt{\frac{1 - Ro^{-2}}{Fr^{-2} - 1}}$$

For large Rossby number the linearity condition writes:

$$h_{max} / d \sqrt{|Fr^{-2} - 1|} \ll 1$$

# The parameterization of subgrid scale orography in LMDz

## 2) Non-linear effects and breaking

Neutral or Fast Flows :  $Fr^{-1} = \frac{N d}{U} \ll 1$

The linearity condition becomes  
(for large Rossby number)  $h_{max} / d \sqrt{|Fr^{-2} - 1|} \sim \frac{h_{max}}{d} = S \ll 1$

Nonlinear dynamics for  $S = h_{max}/d \sim 0(1)$

Streamlines from a 2D Neutral Simulations  
From Wood and Mason (QJ 1993)

$$S = 0.2, Fr^{-1} = 0$$

Note the separation streamline

Hydrodynamic « bluff body » drag:

$$Dr \sim \rho C_d \frac{h_{max}}{d} \frac{U|U|}{2}$$

(if the valley is ventilated!)

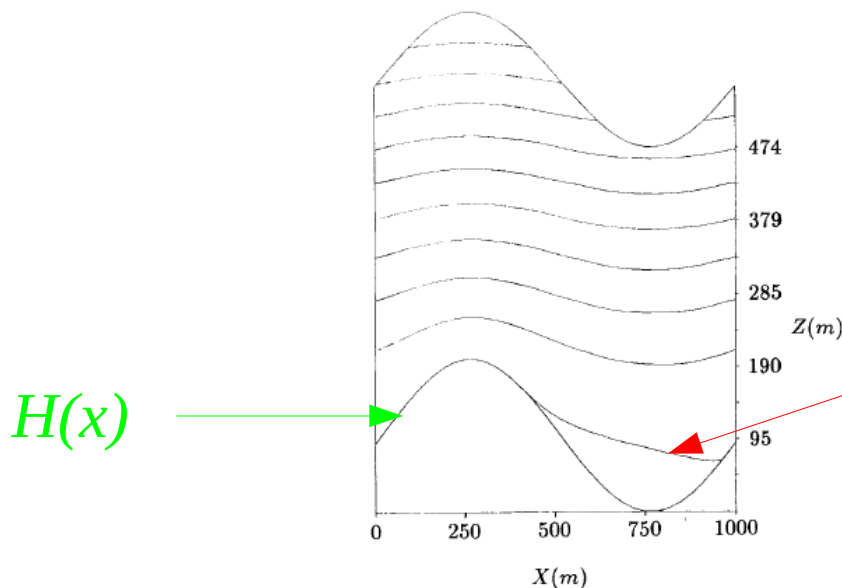


Figure 1. The model-derived streamlines for flow over the two-dimensional hill with  $h = 200$  m ( $\lambda = 1000$  m and  $Z_0 = 0.1$  m). The vertical axis is linear in height above the upstream surface. The horizontal axis shows distance from the point on the upstream slope at which the hill height is half of its maximum value. A separation streamline is clearly visible.

# The parameterization of subgrid scale orography in LMDz

## 2) Non-linear effects and breaking

Neutral or Fast Flows :  $Fr^{-1} = \frac{N d}{U} \ll 1$

Nonlinear dynamics for  $S = h_{max}/d \sim 0(1)$

The dynamics at these scales explain the formation of the « banner » clouds alee of elevated and narrow mountain ridges (Reinert and Wirth, BLM 2009)

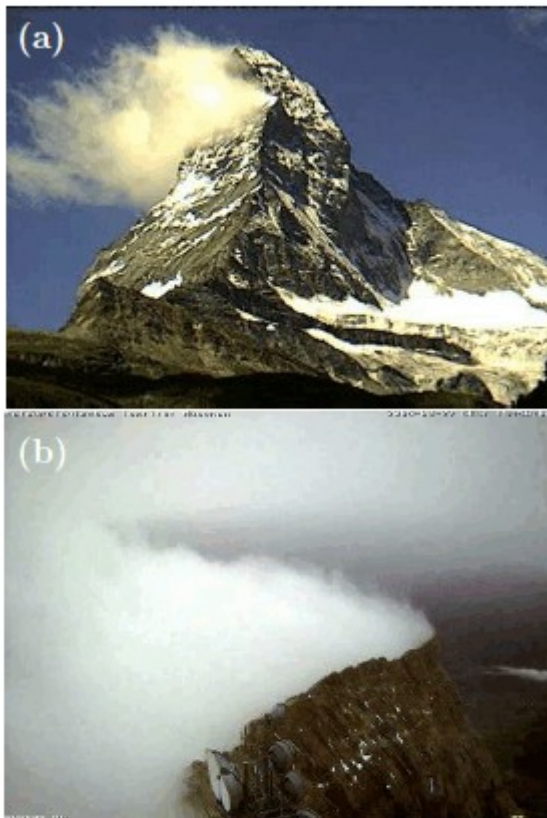
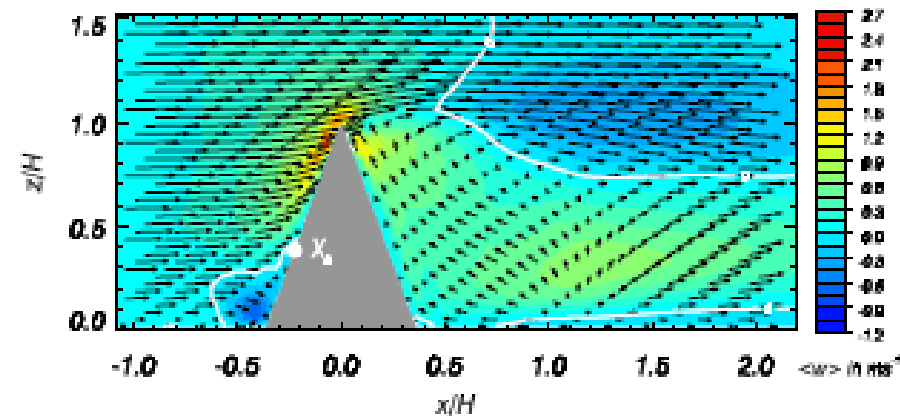


**Figure 1:** Banner clouds forming leeward of a pyramidal shaped mountain peak or a quasi 2D ridge. (a) Banner cloud at Matterhorn (Switzerland). (b) Banner cloud at Mount Zugspitze (Bavarian Alps). Mean flow from right to left.



Large eddy simulation

# The parameterization of subgrid scale orography in LMDz

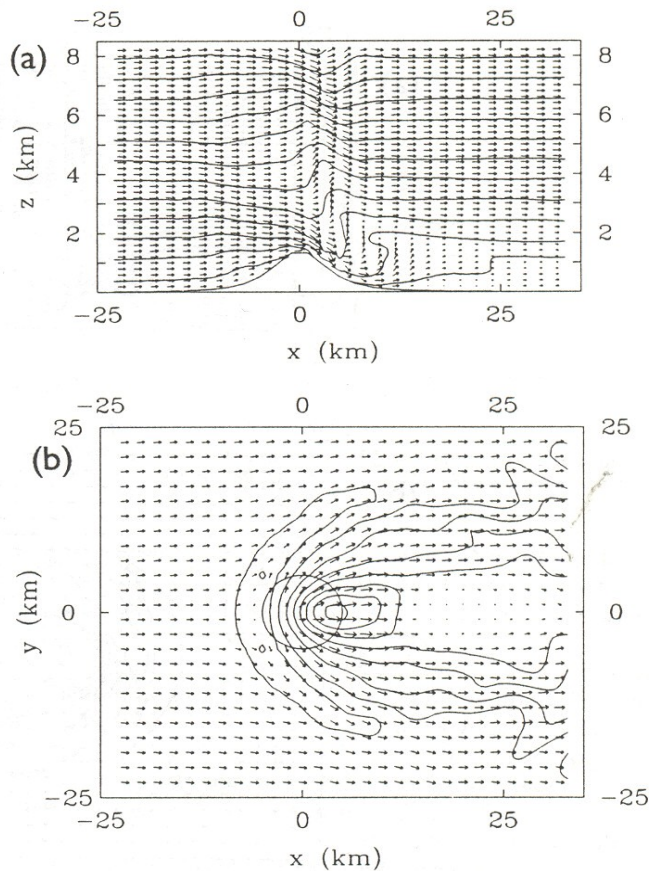
## 2) Non-linear effects and breaking

Stratified or « slow » Flows :  $Fr^{-1} = \frac{N d}{U} \gg 1$

The linearity condition becomes  
(for large Rossby number)

$$h_{max} / d \sqrt{|Fr^{-2} - 1|} \sim \frac{h_{max} N}{U} = H_{ND} \ll 1$$

$H_{ND}$  is the non-dimensional mountain height, again it is almost never small!



Single obstacle simulation with  $h \sim 1\text{km}$ ,  
 $U = 10\text{m/s}$ ,  $N = 0.01\text{s}^{-1}$  :  $H_{ND} = 1$  !  
(Miranda and James 1992)

Note:

Quasi vertical isentropes at low level downstream:  
wave breaking occurs.

The strong Föhn at the surface downstream

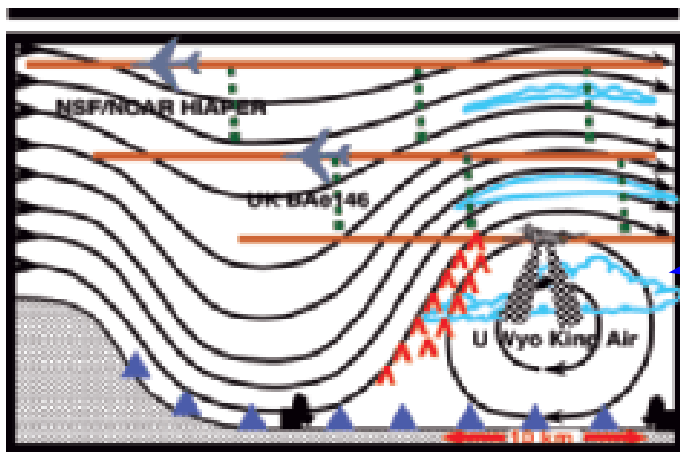
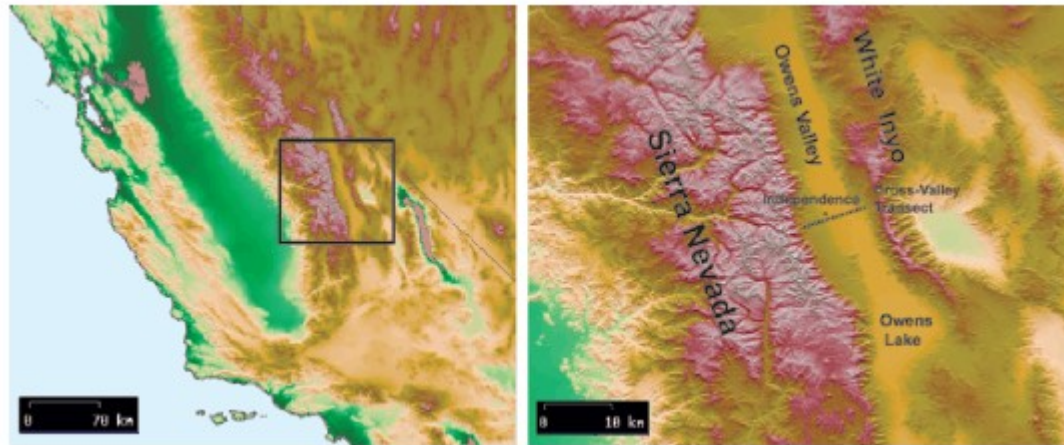
Residual GWs propagating aloft

Apparent slow down near the surface downstream,  
And over a long distance

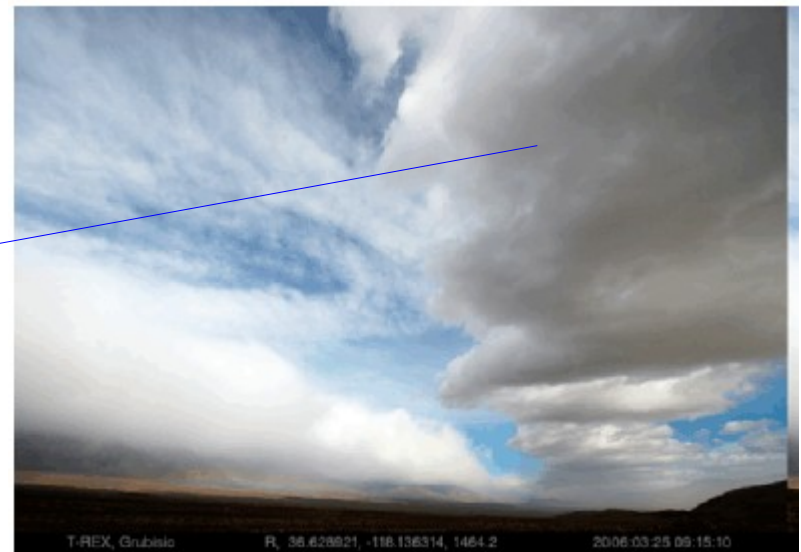
# The parameterization of subgrid scale orography in LMDz

## 2) Non-linear effects and breaking

When low level trapping and low level wave breaking mixes :  
Rotors (T-REX campaign, 2006, Grubisich et al. 2008)



- ground-based lidars
- surface stations
- dropsondes
- jet aircraft
- turbo-prop aircraft with cloud radar turbulence



# The parameterization of subgrid scale orography in LMDz

## 2) Non-linear effects and breaking

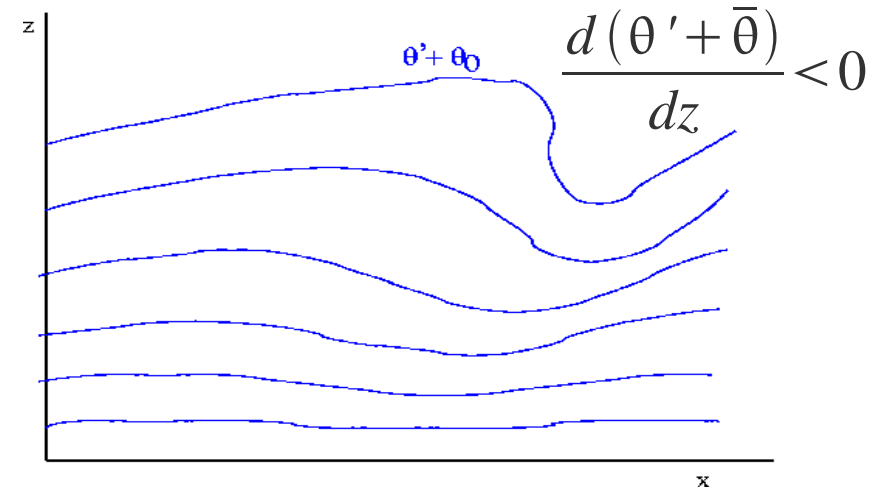
Upper level breaking  
(hydrostatic formalism to allow variations of density with altitude):

$$\left| \hat{\Phi}_{zz} + \frac{\kappa}{H} \hat{\Phi}_z \right| e^{z/2H} > N^2$$

Or by using a WKB formalism:

$$|\hat{w}| < \left| \frac{\hat{\omega}}{m} \right| e^{-z/2H} = w_s(z)$$

$\hat{\omega} = kU$ ,  $\rho_0 = e^{-z/H}$  are the intrinsic frequency and the density, respectively



$$|\overline{F^z}| < |\overline{F_s^z}| \quad \text{ou} \quad \overline{F_s^z} = -\frac{\rho_r \hat{\omega}^3}{2k^2 N} e^{-z/H}$$

**No fluxes through critical levels**

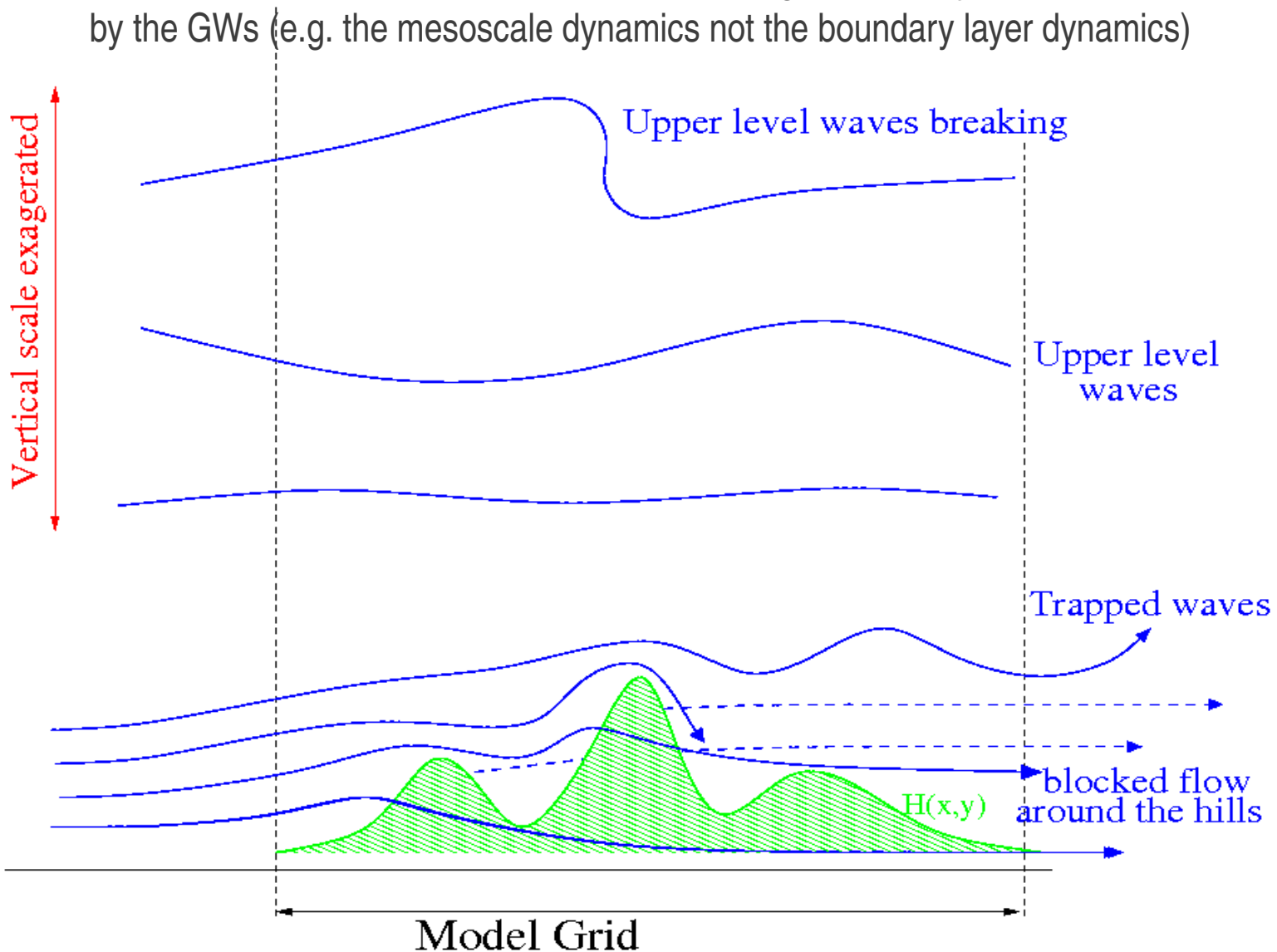
For a constant flow, the breaking altitude is:

$$Z_{br} = 2H \ln \left( \frac{\hat{\omega}^2}{Nk|\hat{w}(0)|} \right)$$

# The parameterization of subgrid scale orography in LMDz

## 3) Formulation of a parameterization

The Lott and Miller (1997) scheme treats the Subgrid Scale Dynamics controlled by the GWs (e.g. the mesoscale dynamics not the boundary layer dynamics)

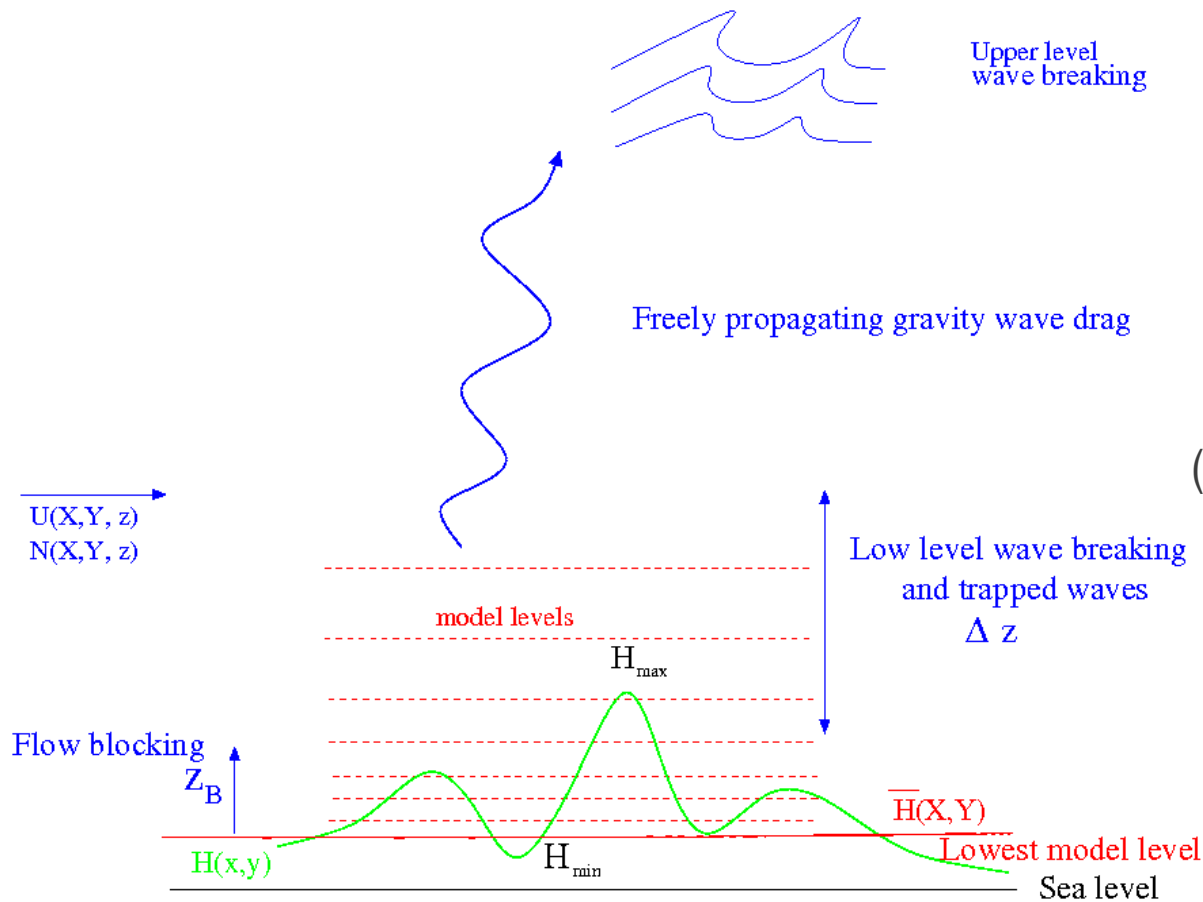




# The parameterization of subgrid scale orography in LMDz

## 3) Formulation of a parameterization

The scheme relies on few non-dimensional parameters, all of Order 1, and which are tunable to a certain extent



Breaking based on a total Richardson number criteria (**Ric**):

Gravity wave drag (**G**)

$$\rho G N U (H_{SSO} - Z_B)^2$$

If breaking is diagnosed at low level (between  $Z_B$  and  $Z_B + \Delta Z$ ), a fraction of the drag is

distributed over  $\Delta Z$ :

$$\int_{Z_B}^{Z_B + \Delta Z} \frac{N}{U} dz < \frac{\pi}{2}$$

Flow blocking (**H<sub>NC</sub>**)

$$\int_{Z_B}^{H_{max}} \frac{N}{U} dz < H_{NC}$$

# The parameterization of subgrid scale orography in LMDz

## 3) Formulation of a parameterization

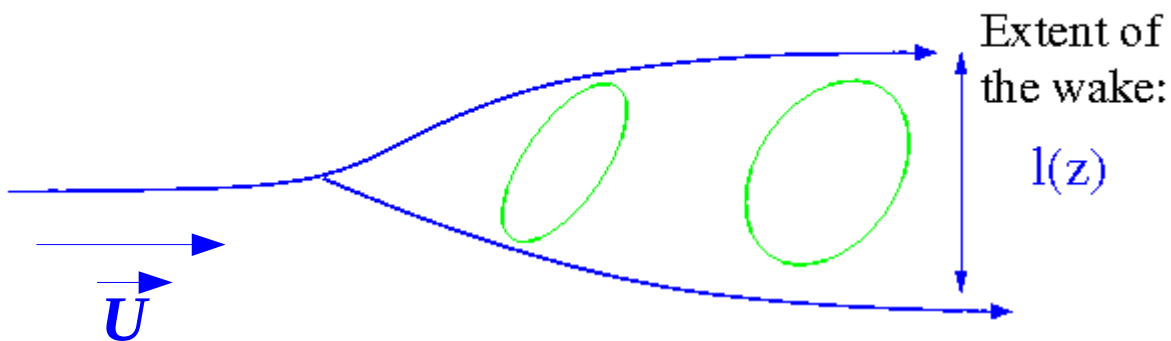
The scheme relies on few non-dimensional parameters, all of Order 1, and which are tunable to a certain extent

A arbitrary fraction of the drag (around 50%) is also deposited in the low troposphere to represent trapped lee waves.

Blocked flow drag is applied below  $Z_B$  ( **$Cd$** ):

Bluff body drag applied at each model layer that intersects the Subgrid Scale Orography (SSO):

Below  $Z_B$



$$D_B = \rho l(z) C_d \frac{\vec{U} \|\vec{U}\|}{2}$$

# The parameterization of subgrid scale orography in LMDz

## 3) Formulation of a parameterization

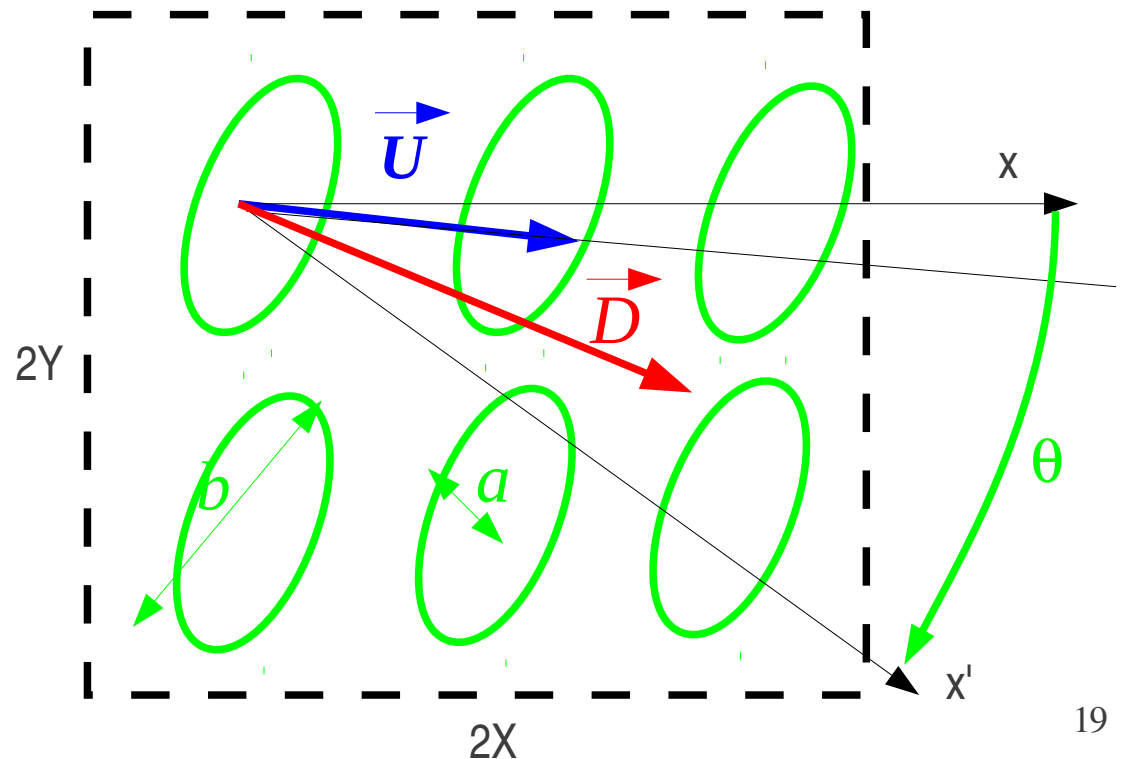
The scheme also takes into account the anisotropy of mountains, with the direction of the drags in between the direction of the flow and the minor axis of the mountains.

We include this anisotropic effect by modelling the SSO as ensemble of elliptical mountains uniformly distributed over the model grid

For anisotropic mountains, the wave drag direction at the surface is in between the direction of the flow and the direction of max descent of the mountain

For one elliptic mountain formulae are in Phillips (1984)

$$H = \frac{H_0}{1 + \frac{x'^2}{a^2} + \frac{y'^2}{b^2}}$$



# The parameterization of subgrid scale orography in LMDz

## 3) Formulation of a parameterization

We have to express the formulae in Phillips (1985) by evaluating  $H_0$ ,  $a$ ,  $b$ , the angle  $\theta$ , the number of ridges in the gridbox  $N_{ridges} \sim ab/(XY)$ ....

They are related to statistics of the SSO elevation evaluated from a high resolution orography database that gives:

the variance  $\mu$ , the slope  $\sigma$ , the angle  $\theta$ , and the anisotropy  $\gamma$ .

For one mountain:

$$H = \frac{2\mu^3}{\mu^2 + \sigma^2 x'^2 + \gamma^{-2} \sigma^2 y'^2}$$

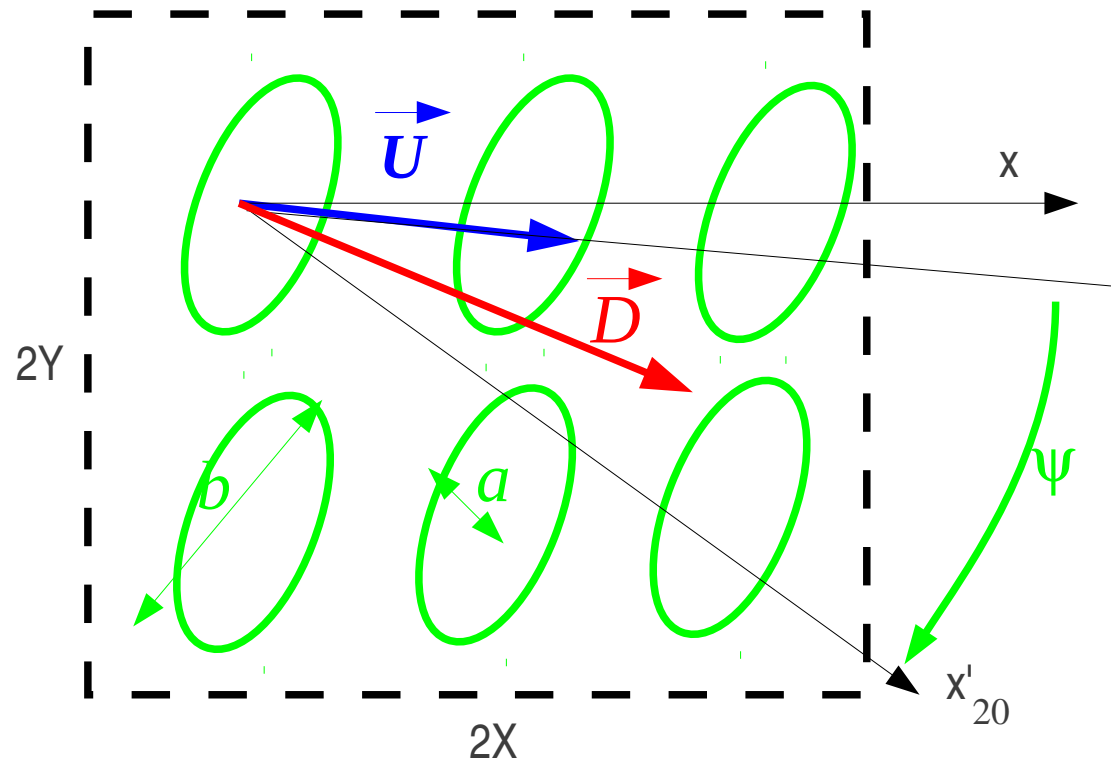
For  $N_{ridges}$  the drag vector becomes:

$$D_{x'} = \rho U N \mu \sigma G (B \cos^2 \psi + C \sin^2 \psi)$$

$$D_{y'} = \rho U N \mu \sigma G (B - C) \cos \psi \sin \psi$$

From Phillips (1985):

$$B = 1 - 0.18\gamma - 0.04\gamma^2, C = 0.48\gamma + 0.3\gamma^2$$

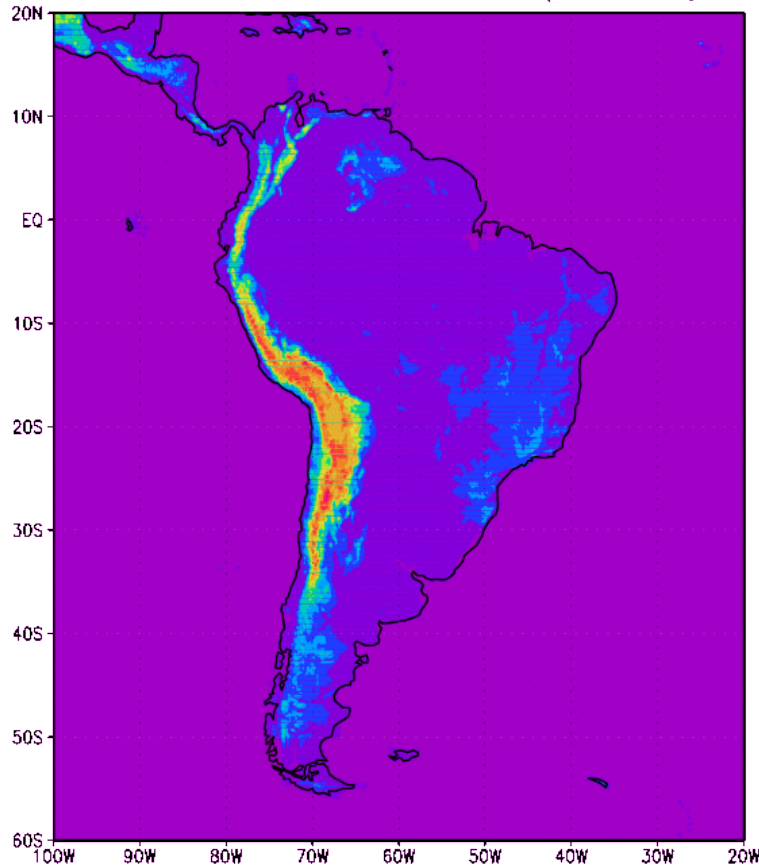


# The parameterization of subgrid scale orography in LMDz

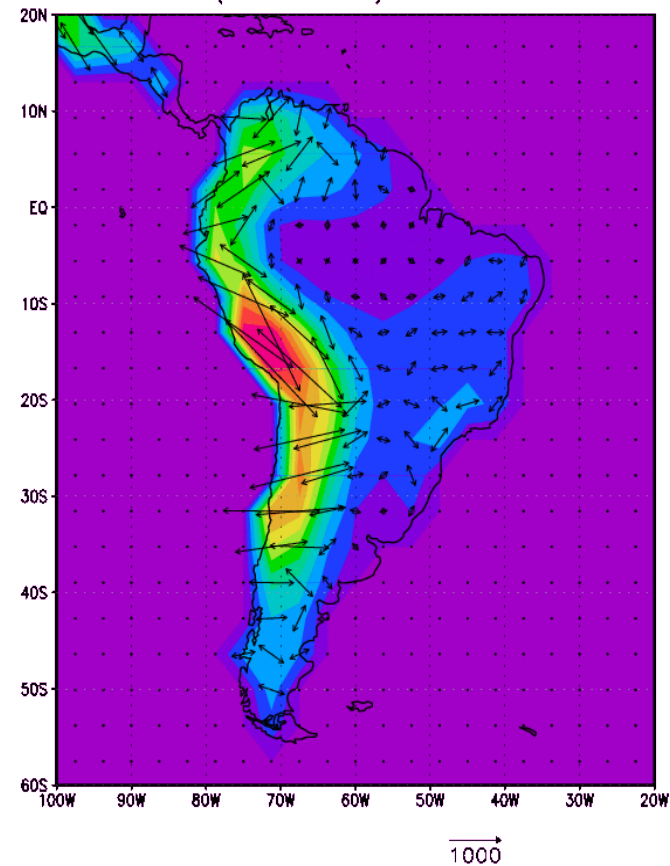
## 3) Formulation of a parameterization

All the subgrid parameters,  $H_{\min}$ ,  $H_{\max}$ ,  $\mu$ ,  $\sigma$ ,  $\theta$ , and  $\gamma$  are build from statistics of measured mountain elevations

H from USN database (10'x10')



Std. Dev (CI=100m) and Orientation



GCM with 2.5°x2.5° grid

# The parameterization of subgrid scale orography in LMDz

## 4) Validation and test in a NWP model

There are 2D and 3D theoretical simulations for uniform flows over mountains

2D, Stein (1992)

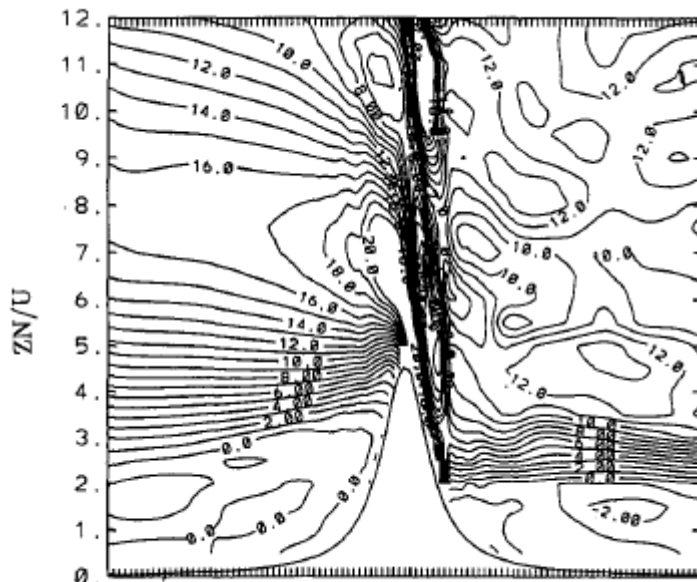
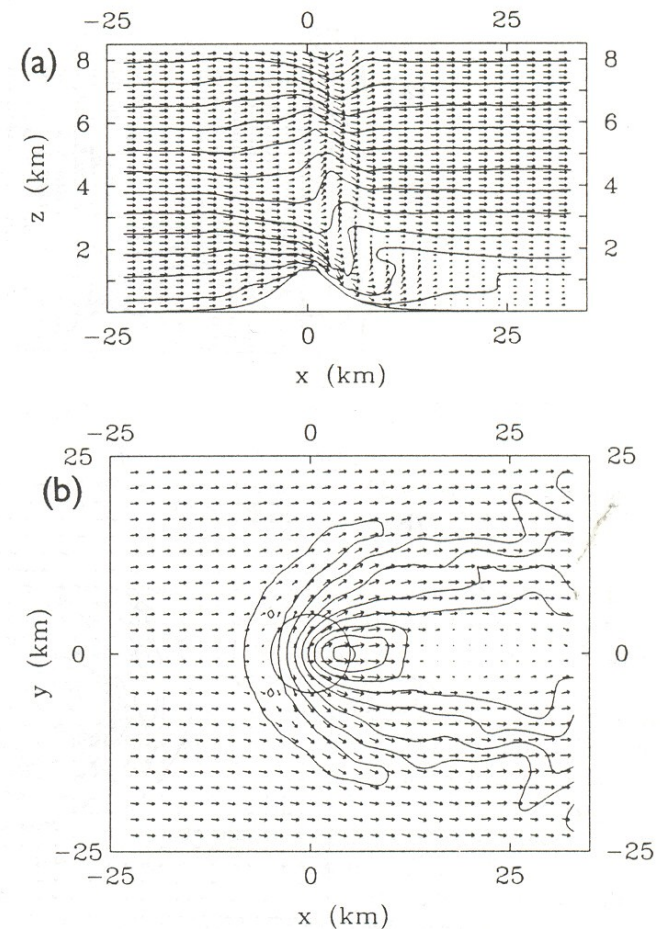


FIG. 9. Horizontal wind at  $t_* = 20$  for  $F = 4.5$ ,  $S = 0.01$ .

3D, Miranda and James (1992)



# The parameterization of subgrid scale orography in LMDz

## 4) Validation and test in a NWP model

There are 2D and 3D theoretical simulations for uniform flows over mountains,  
The scheme can be used to predict the drag in those simulations  
(Lott and Miller 1997).

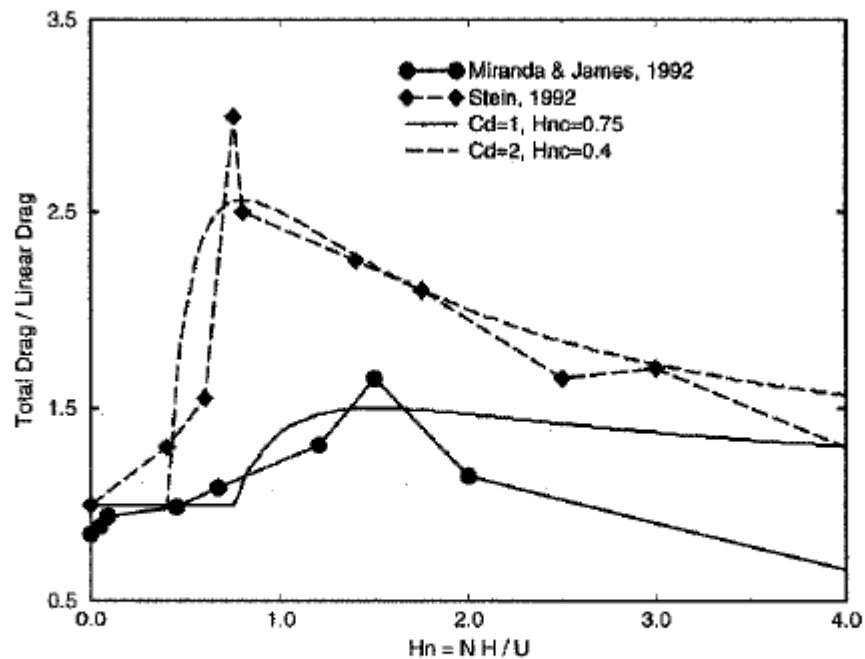


Figure 2. Ratio between the total mountain drag and the linear gravity-wave drag as a function of  $H_n$ . The continuous line and the dotted line correspond to the drag ratio predicted by the conceptual model upon which the new subgrid-scale orographic drag scheme is based. The dotted line with diamond symbols corresponds to values found in 2-D nonlinear simulations (Stein 1992). The continuous line with circle symbols correspond to values found in 3-D nonlinear simulations (Miranda and James 1992).

# The parameterization of subgrid scale orography in LMDz

## 4) Validation and test in a NWP model

There are field experiments, where the surface drag was measured by arrays of micro-barographs, and in some occasion, the wave momentum fluxes by Airplanes.

For the Pyrénées and the ECMWF forecast model, we have used the Pyrex data (Bougeault et al. 1992)

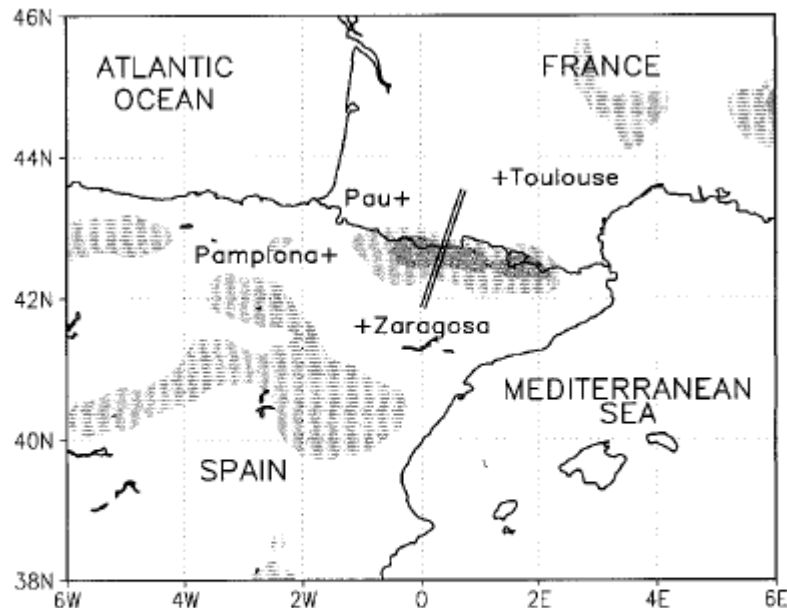


FIG. 1. Smoothed terrain elevation and PYREX data used. Here, + denotes the location of the high-resolution soundings. The two thick lines indicate the airplane paths during the IOP 3. The light- and dark-shaded areas denote terrain elevation above 1000 m and 1500 m, respectively.

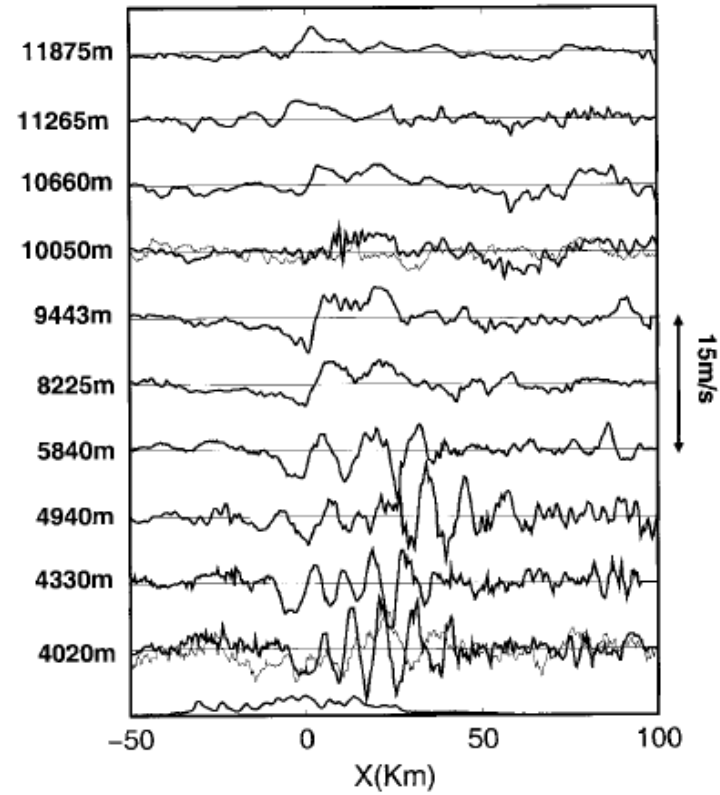


FIG. 2. Observed vertical velocities from different aircraft legs, from 15 Oct 1990 around 0600 UTC. Thick lower curve represents the Pyrénées; the thin curve at the  $Z = 4$  km and  $Z = 10$  km are red-noise surrogates with characteristics adapted to the measured vertical velocity at that level.



# The parameterization of subgrid scale orography in LMDz

## 4) Validation and test in a NWP model

There are field experiments, where the surface drag was measured by arrays of micro-barographs, and in some occasion, the wave momentum fluxes by Airplanes.

At a truncature T106, typical of the GCMs used today in the Earth System Models, The SSO drag scheme makes up the total drag due to the Pyrénées (the resolution is too coarse to see this mountain explicitly).

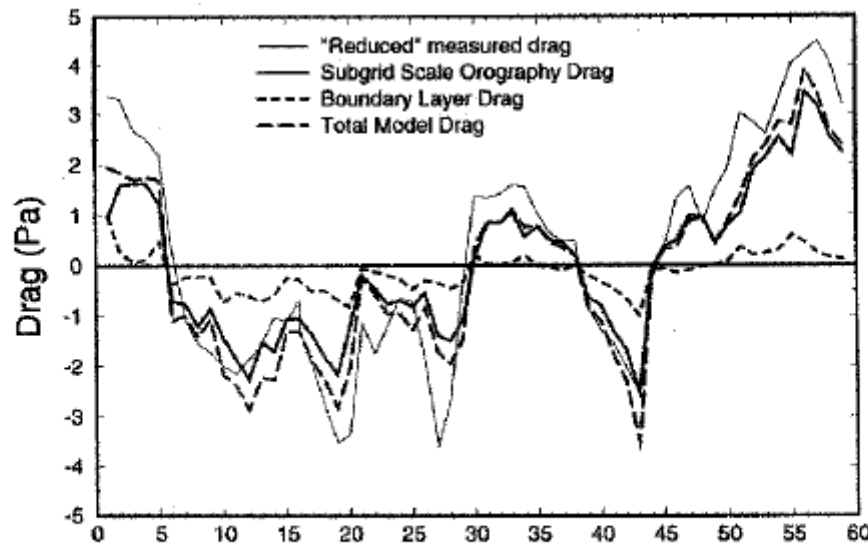


Figure 8. T106 forecasts: ECMWF model with mean orography and the new subgrid-scale orographic drag scheme. Parametrized mountain drags during PYREX. The comparison is limited to the 60 PIO cases defined in the text.

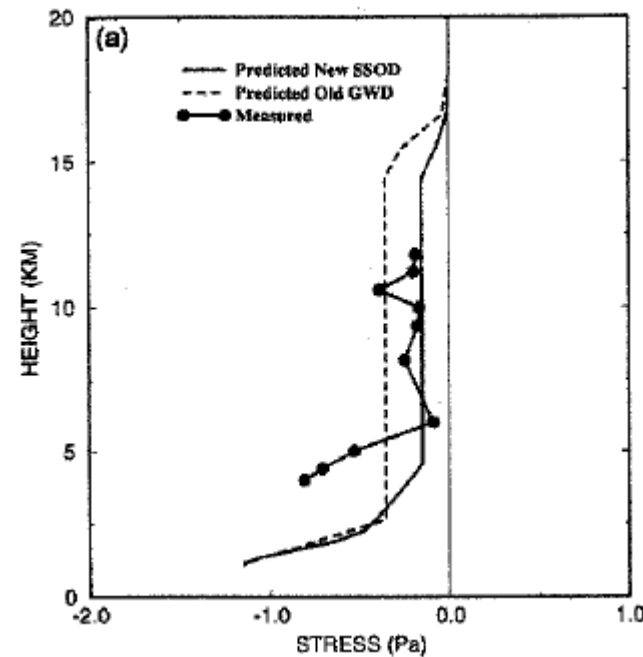
The scheme also improved the ECMWF forecast performances and is still operationnal, it is also operationnal at the Max-Planck Institute

# The parameterization of subgrid scale orography in LMDz

## 4) Validation and test in a NWP model

The scheme also produce a profil of wave momentum flux aloft the mountain that  
Matches somehow the measured one.

Note that the momentum fluxes are almost an order of magnitude lower than  
the surface drag, which witness that a lot occurs at low level, and that it  
was sounded to consider this low level effect explicetely into the scheme



# The parameterization of subgrid scale orography in LMDz

## 4) Validation and test in a NWP model

The effect of the low level drag is to produce a low level wake, quite in agreement with the higher resolutions forecast and analysis used during the campaign

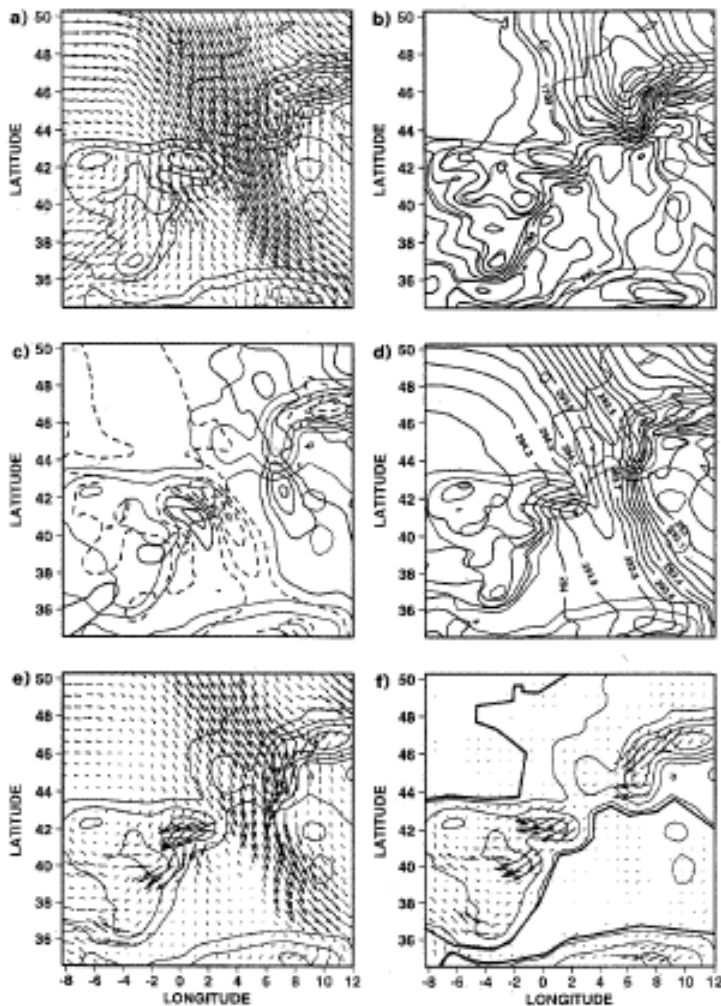


Figure 10. T213 forecast: ECMWF model with mean orography and the new subgrid-scale orographic drag scheme, 15 November 1990 at 6 UTC. Orography (interval: 400 m) and flow diagnostics on the isentropic surface  $\theta = 293 \text{ K}$ . (a) wind; (b) height of isentropic surface, interval: 200 m; (c) isentropic relative vorticity, interval:  $0.5 \times 10^{-4} \text{ s}^{-1}$ ; (d) Bernoulli function, interval:  $100 \text{ J kg}^{-1}$ ; (e) total potential vorticity flux; (f) potential vorticity fluxes due to the parametrized frictional forces and diabatic heating. Coastlines are shown on Fig. 10(f).

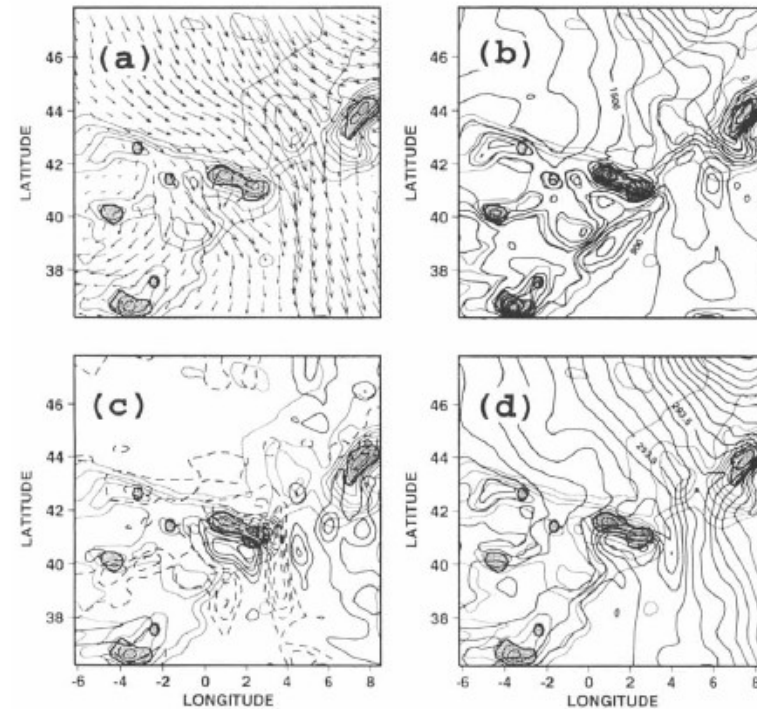


Figure 13. Peridot analysis, 06 UTC 15 November 1990. Orography (contour interval = 400 m) and flow diagnostics on the isentropic surface  $\theta = 293 \text{ K}$ . In the shaded area the isentropic surface goes below the lowest model level. (a) Wind, (b) elevation (contour interval = 200 m), (c) isentropic relative vorticity (contour interval =  $0.5 \times 10^{-4} \text{ s}^{-1}$ , with negative values dashed), and (d) Bernoulli function (contour interval =  $100 \text{ J kg}^{-1}$ ).

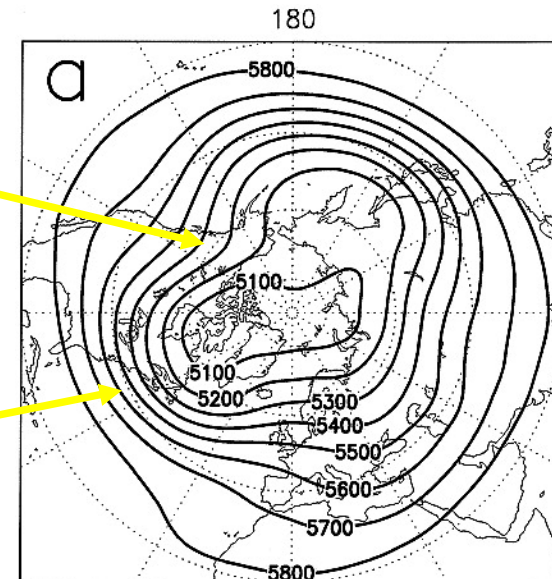
# The parameterization of subgrid scale orography in LMDz

## 5) Impact in a GCM

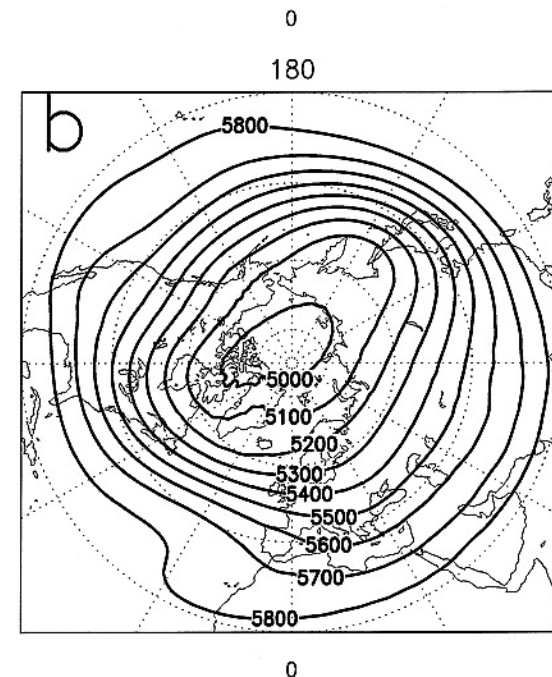
Although the Lott and Miller (1997) SSO drag scheme improve the performances of the ECMWF forecasts (e.g. few days simulations), it does not improve the structure of the steady planetary waves in climate simulations.

Ridges ( $\xi < 0$ )

Troughs ( $\xi > 0$ )



NCEP

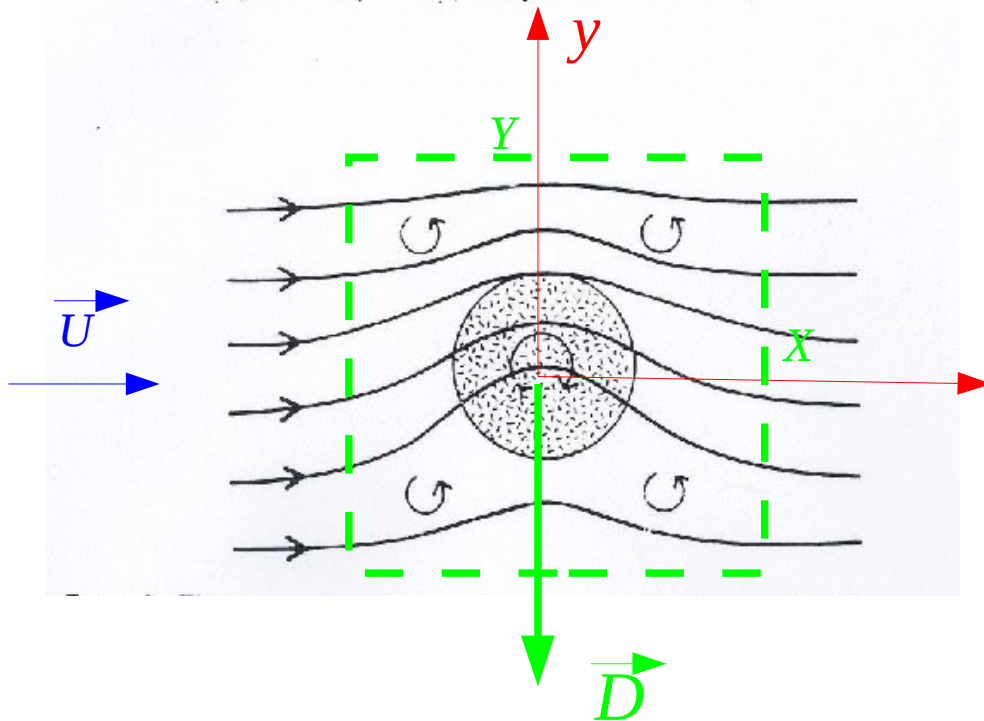
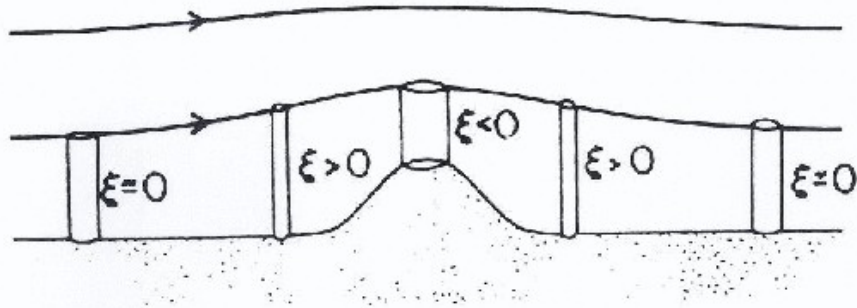


LMDz  
old  
version

# The parameterization of subgrid scale orography in LMDz

## 5) Impact in a GCM

To fix this problem remember that the forcing of the planetary waves by mountains is essentially due to vortex stretching ! A process that is associated to a large lift force.



During vortex stretching in the midlatitudes

The mountain felt the background pressure meridional gradient in geostrophic equilibrium with the background wind :

$$P = P_s - f U y$$

$$\vec{D} = \frac{1}{4XY} \int_{-Y}^Y \int_{-X}^X + H \vec{\nabla} p \, dx \, dy$$

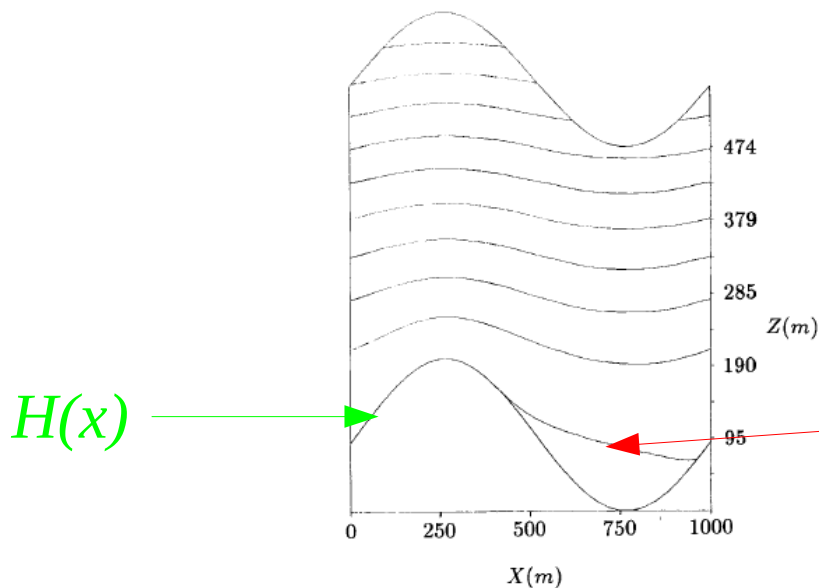
In the linear case:

$$\vec{D} = \vec{L} = -\rho f U \bar{H} \vec{y}$$

# The parameterization of subgrid scale orography in LMDz

## 5) Impact in a GCM

A reason for which the models that use mean orographies at the lower boundary may underestimate the lift force, because they neglect that the air in valleys can be quite isolated from the large scale circulation.



Streamlines from a 2D Neutral Simulations  
From Wood and Mason (QJ 1993)

$$S=0.2, Fr^{-1}=0$$

Note the separation streamline

Figure 1. The model-derived streamlines for flow over the two-dimensional hill with  $h = 200$  m ( $\lambda = 1000$  m and  $Z_0 = 0.1$  m). The vertical axis is linear in height above the upstream surface. The horizontal axis shows distance from the point on the upstream slope at which the hill height is half of its maximum value. A separation streamline is clearly visible.

# The parameterization of subgrid scale orography in LMDz

## 5) Impact in a GCM

A solution can be to higher up the mountains elevation by a fraction of its variance,  
This the concept of envelop orography (Wallace et al. 1983)

An other is to keep a mean orography and to apply the missing forces directly  
in the models levels that intersect the mountain peaks (Lott 1999).

Lift parameter of order 1 ( $C_l$ )

$$D_l = -\rho C_l f \left( \frac{H_{max} - z}{H_{max} - H_{mean}} \right) \vec{k} \times \vec{U}$$

When integrated from  $H_{mean}$  to  $H_{max}$  this drag gives the Lift stress if  $C_l=2$

# The parameterization of subgrid scale orography in LMDz

## 5) Impact in a GCM

Illustration of those concepts by parametrizing all the mountains by forces in  
A GCM (explicit lower model level stays at sea level!). All maps are  
for geopotential anomalies (e.g. after subtraction of zonal mean values)

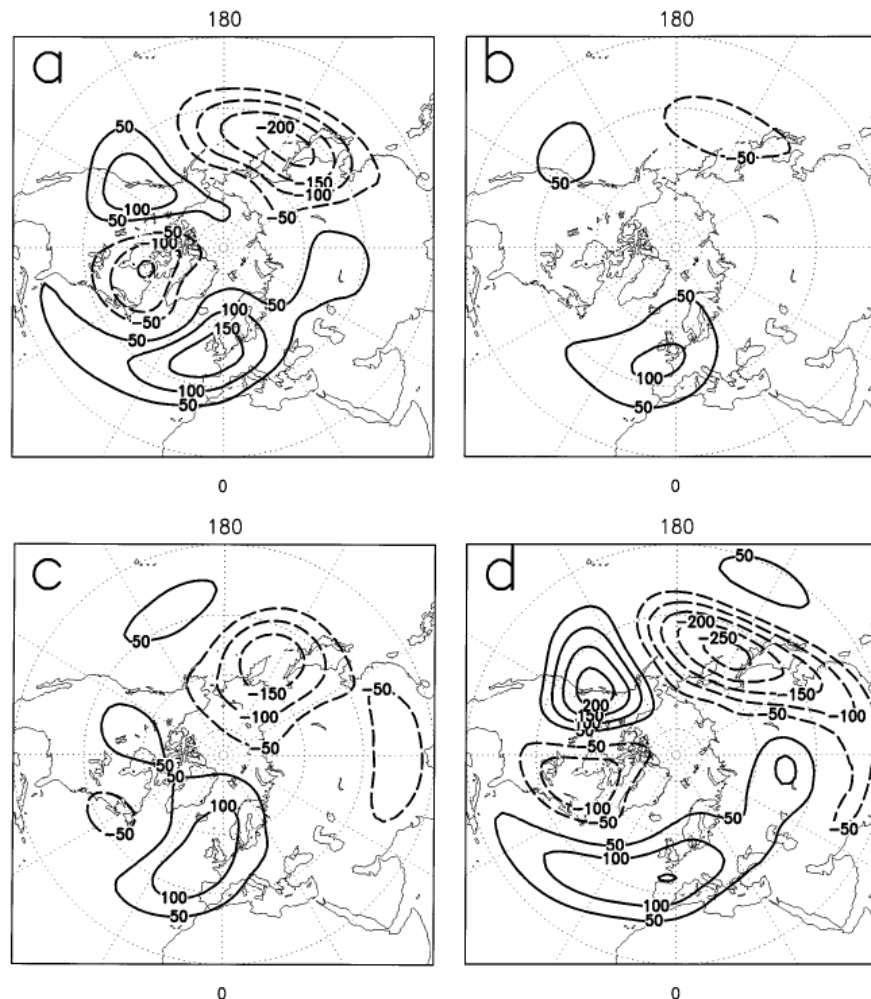


FIG. 3. Anomaly to the zonal mean of the geopotential height at 500 hPa averaged over the winter months (DJF) of the period 1985-90. LMD run with no explicit orography. (a) NMC analysis; (b) LMD no drag, no lift; (c) LMD low drag only; (d) LMD low lift only. Zero line not shown; negative values are dashed.

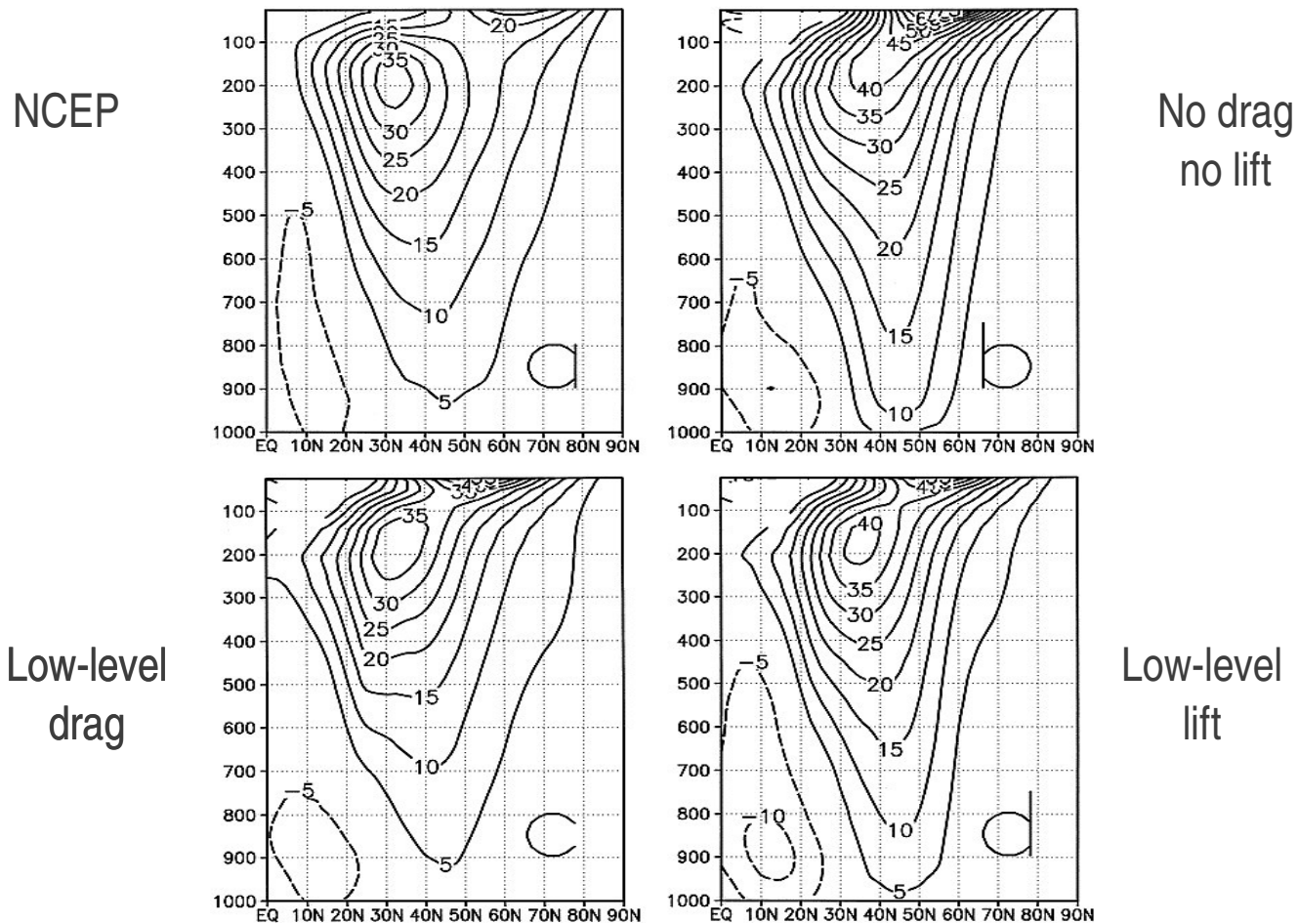


# The parameterization of subgrid scale orography in LMDz

## 5) Impact in a GCM

Testing ideas in model simulations where the mountains are entirely parameterized!

Zonal mean zonal wind in the midlatitudes



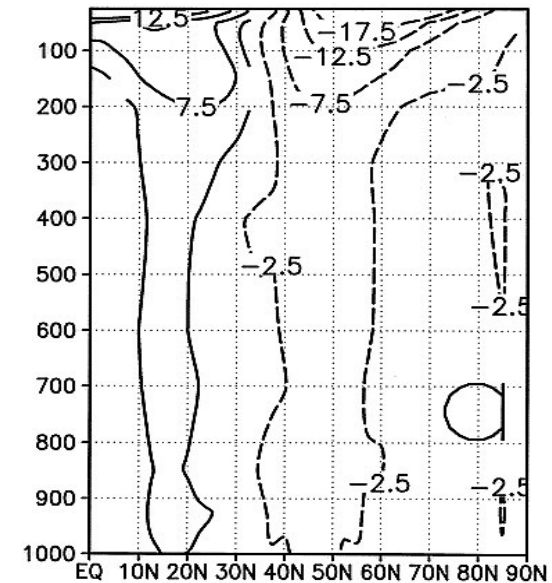
# The parameterization of subgrid scale orography in LMDz

## 5) Impact in a GCM

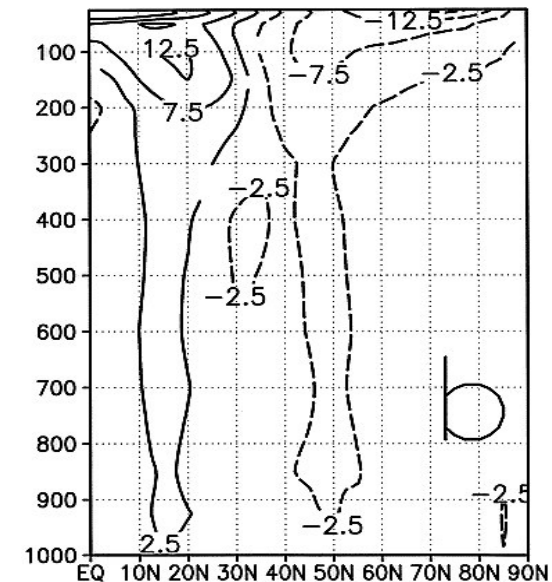
Simulation with mean explicit orography without and with the subgrid scale orographic drag scheme including enhanced lift

Error maps between the zonal wind NCEP reanalysis minus LMDz  
Winter months out of a 10years long simulation

Without



With

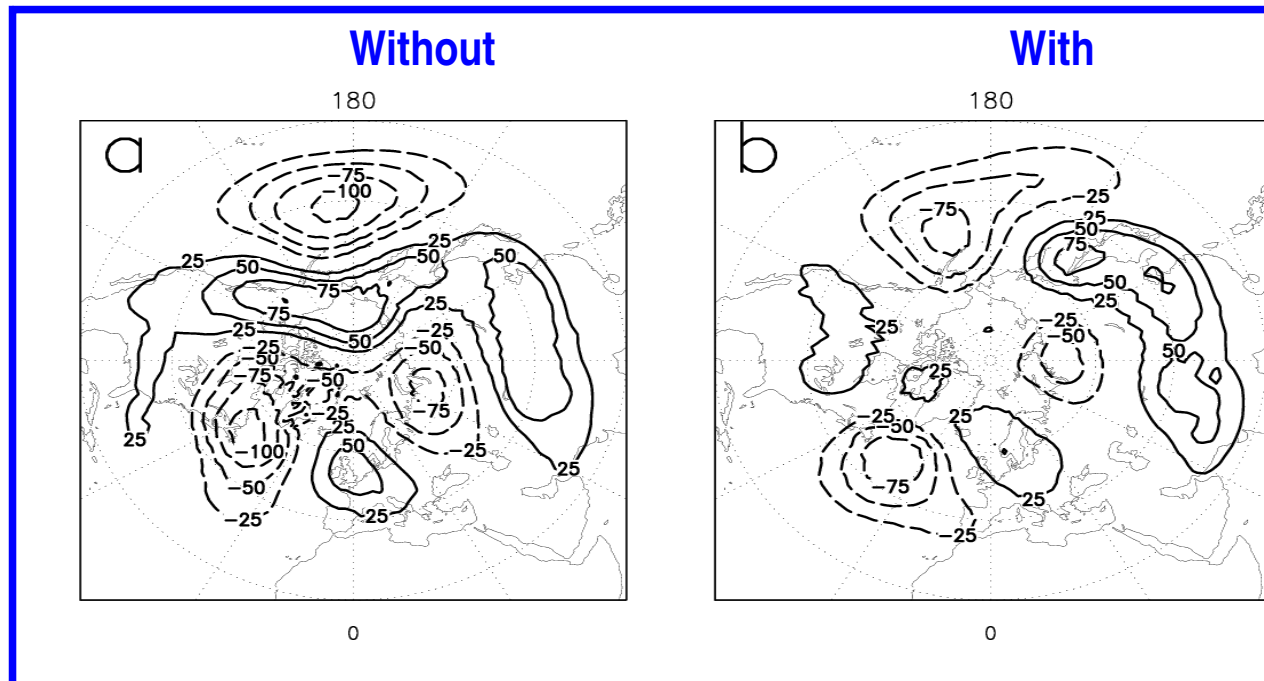


# The parameterization of subgrid scale orography in LMDz

## 5) Impact in a GCM

Simulation with mean explicit orography without and with the subgrid scale orographic drag scheme including enhanced lift

Error maps between the Geopotential height at 700hPa,  
NCEP reanalysis minus LMDz  
Winter months out of a 10years long simulation



# The parameterization of subgrid scale orography in LMDz

## 6) Prospective

- Reconciliate SSO schemes and boundary layer schemes  
(They often do the same things at low level)
- Make SSO schemes more stochastic to treat better a large ensemble of waves  
(3D-Critical levels and trapped waves need that, if significant....)
- Evaluate impact on synoptic scale flows (cold surges, lee cyclogenesis.....)